

2

AD-A253 565



DTIC
ELECTE
AUG 4 1992
S C D

SMART ARMOR CONCEPTUAL DESIGN
FINAL TECHNICAL REPORT

By:

- K. V. Logan
- S. N. Atluri
- S. V. Hanagud
- W. L. Ohlinger
- G. R. Villalobos

April 30, 1992

U. S. ARMY RESEARCH OFFICE
CONTRACT NO. DAAL03-91-G-0300

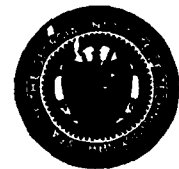
Materials Science and Technology Laboratory
Computational Mechanics Research Center
School of Aerospace Engineering

UNCLASSIFIED
DATE 01-12-2001 BY 60322 UCBAW

GEORGIA INSTITUTE OF TECHNOLOGY

A Unit of the University System of Georgia
Atlanta, Georgia 30332

Georgia Tech
RESEARCH INSTITUTE



92-20882



THE VIEWS, OPINIONS, AND/OR FINDINGS CONTAINED IN THIS REPORT
ARE THOSE OF THE AUTHORS AND SHOULD NOT BE CONSTRUED AS AN
OFFICIAL DEPARTMENT OF THE ARMY POSITION, POLICY, OR
DECISION, UNLESS SO DESIGNATED BY OTHER DOCUMENTATION

TABLE OF CONTENTS

LIST OF ILLUSTRATIONS	iii
LIST OF TABLES	iv
ABSTRACT	1
I. SCOPE OF WORK	2
II. BACKGROUND	3
II.1 What Is Smartness?	3
II.2 Current Applications and Examples	4
III. SUMMARY OF MOST IMPORTANT RESULTS	5
III.1 Order of Magnitude Determinations	5
III.2 Smart Actuation to Preserve Armor Integrity	16
III.3 Microactuators and their Application to Smart Armors	38
III.4 Smart Armors to Defeat Projectiles	53
III.5 Smart Reacting Armor	60
III.6 Energy Absorption Structure	63
III.7 Dilatant Material	64
III.8 Broken Shells	65
III.10 Electromigration	69
IV. LIST OF PARTICIPATING SCIENTIFIC PERSONNEL	70
VI. RECOMMENDATIONS	71
BIBLIOGRAPHY	73

LIST OF ILLUSTRATIONS

		<u>Page</u>
Figure III.1.1	Case 1: Battle Tank Against Anti-Tank Long Rod Projectile.	13
Figure III.1.2	Case 2: Aircraft Armor Against Anti-Aircraft Projectile.	14
Figure III.1.3	Case 3: Tank/Turret Armor Against Missiles.	15
Figure III.2.1	Flow Chart for Running Pisces-2 DELK.	22
Figure III.2.2	Mesh Plot Showing Grid Scheme for Projectile and Armor.	23
Figure III.2.3	Distortion Contour After 200 Cycles.	24
Figure III.2.4	Distortion Contour After 400 Cycles.	25
Figure III.2.5	Distortion Contour After 600 Cycles.	26
Figure III.2.6	Distortion Contour After 800 Cycles.	27
Figure III.2.7	Stress Contour After 800 Cycles.	28
Figure III.2.8	Stress Contour After 800 Cycles With Lower Portion of the Armor Supported.	29
Figure III.2.9	Stress Contour After 100 Cycles With Smart Actuation.	30
Figure III.2.10	Stress Contour After 100 Cycles With Smart Actuation.	31
Figure III.2.11	Stress Contour After 100 Cycles With Smart Actuation.	32
Figure III.2.12	Stress Contour After 100 Cycles With Smart Actuation.	33
Figure III.2.13	Stress Contour After 100 Cycles With Smart Actuation.	34
Figure III.2.14	Stress Contour After 100 Cycles With Smart Actuation.	35
Figure III.2.15	Stress Contour After 100 Cycles With Smart Actuation.	36
Figure III.2.16	Stress Contour After 800 Cycles With Smart Actuation.	37
Figure III.3.1	A Schematic of an Electrostatic Micromotor.	43
Figure III.3.2	Top and Cross-Sectional Views of a Micromotor.	44
Figure III.3.3	Shape Memory Alloy as a Micromotor.	45
Figure III.3.4	A Typical Induced Drive Mechanism.	46
Figure III.3.5	Ceramic Plate.	47
Figure III.3.6	Setup for the Microactuation.	48
Figure III.3.7	Distortion Plot After First Cycle.	49
Figure III.3.8	Distortion Plot After Second Cycle.	50
Figure III.3.9	Distortion Plot After Third Cycle.	51
Figure III.3.10	Distortion Plot After 10 Cycles.	52
Figure III.4.1	A Military Vehicle With Sloping Armor.	56
Figure III.4.2	A Control Mechanism.	57
Figure III.4.3	Block Diagram.	58
Figure III.4.4	An Experimental Set-Up for ER-Fluid.	59

LIST OF ILLUSTRATIONS (cont'd)

	<u>Page</u>
Figure III.5.1 Two Stage Projectile.	61
Figure III.5.2 Application of Microactuation Concepts in Smart Armor.	62

LIST OF TABLES

	<u>Page</u>
TABLE I. Description of Various Cases Considered for Calculation	7
TABLE II. (for Case 1)	8
TABLE III. (for Case 2)	9
TABLE IV. (for Case 3)	10
TABLE V. Appendix	11

SMART ARMOR CONCEPTUAL DESIGN
FINAL TECHNICAL REPORT

By:

K. V. Logan
S. N. Atluri
S. V. Hanagud
W. L. Ohlinger
G. R. Villalobos

April 30, 1992

U. S. ARMY RESEARCH OFFICE
CONTRACT NO. DAALO3-91-G-0300

Materials Science and Technology Laboratory
Computational Mechanics Research Center
School of Aerospace Engineering

Georgia Institute of Technology
Atlanta, Georgia 30332

APPROVED FOR PUBLIC RELEASE
DISTRIBUTION UNLIMITED

DTIC QUALITY INSPECTED 5

Approved For	
DTIC QUALITY	<input checked="" type="checkbox"/>
DTIC FILE	<input type="checkbox"/>
Documentation	<input type="checkbox"/>
Justification	
Distribution/	
Availability Codes	
Avail and/or	
Dist Special	
A-1	

REPORT DOCUMENTATION PAGE

Form Approved
OMB No. 0704-0188

Public reporting burden for this collection of information is estimated to average 1 hour per response, including the time for reviewing instructions, searching existing data sources, gathering and maintaining the data needed, and completing and reviewing the collection of information. Send comments regarding this burden estimate or any other aspect of this collection of information, including suggestions for reducing this burden, to Washington Headquarters Services, Directorate for Information Operations and Reports, 1215 Jefferson Davis Highway, Suite 1204, Arlington, VA 22202-4302, and to the Office of Management and Budget, Paperwork Reduction Project (0704-0188), Washington, DC 20503

1. AGENCY USE ONLY (Leave blank)	2. REPORT DATE 30 April 92	3. REPORT TYPE AND DATES COVERED FINAL 1 Apr 91 - 29 Jul 92
---	--------------------------------------	---

4. TITLE AND SUBTITLE Smart Armor Conceptual Design	5. FUNDING NUMBERS
---	---------------------------

6. AUTHOR(S) K. V. Logan, S. N. Atluri, S. V. Hanagud, W. L. Ohlinger, G. R. Viilalobos	5. FUNDING NUMBERS DAAL03-91-G-0300
--	---

7. PERFORMING ORGANIZATION NAME(S) AND ADDRESS(ES) Georgia Institute of Technology Atlanta, GA 30332	8. PERFORMING ORGANIZATION REPORT NUMBER GIT No. A-9034-000
---	--

9. SPONSORING / MONITORING AGENCY NAME(S) AND ADDRESS(ES) U. S. Army Research Office P. O. Box 12211 Research Triangle Park, NC 27709-2211	10. SPONSORING / MONITORING AGENCY REPORT NUMBER ARO 29317.1-EG
--	---

11. SUPPLEMENTARY NOTES
The view, opinions and/or findings contained in this report are those of the author(s) and should not be construed as an official Department of the Army position, policy, or decision, unless so designated by other documentation.

12a. DISTRIBUTION / AVAILABILITY STATEMENT Approved for public release; distribution unlimited.	12b. DISTRIBUTION CODE
---	-------------------------------

13. ABSTRACT (Maximum 200 words)

This Final Report is a summary of an eight months effort to determine the feasibility of concepts to design a responsive, resilient armor. Unique materials, armor systems and applications of new technologies to smart armors capable of enhanced ballistic protection and self-healing have been conceptualized and studied to establish feasibility. The promise for such concepts appears excellent, but much work remains to establish the optimum designs and develop them into usable armor systems.

The concepts explored range from passive systems in which unique (to armor) materials properties, such as solid-liquid phase transformations, would be used to maximize energy dissipation; to active concepts, in which micromotors would be used to modify the stress distribution in a favorable fashion, leading to enhanced projectile defeat capability; to concepts in which the armor material would assess the level of damage inflicted by a ballistic impact, and would then "heal" that damage to provide at least a minimal level of protection against additional attack.

Additional concepts of sensing and actuation are explored and unique applications of these traditional smart material concepts to armor are conceptualized.

Modeling of ballistic impact phenomena has been performed using the Pisces program, and limited results are presented indicating the worth of modifying the interaction between stress waves and material surfaces. This is a critical capability in the context of further work, which will use such modelling extensively to investigate such approaches prior to actual experimentation.

14. SUBJECT TERMS Armor, Smart Materials, Sensors, Actuators, Micromotors, Shape Memory Alloys, Ballistic Impact, Titanium Diboride, Ceramics, Piezoelectrics	15. NUMBER OF PAGES
	16. PRICE CODE

17. SECURITY CLASSIFICATION OF REPORT UNCLASSIFIED	18. SECURITY CLASSIFICATION OF THIS PAGE UNCLASSIFIED	19. SECURITY CLASSIFICATION OF ABSTRACT UNCLASSIFIED	20. LIMITATION OF ABSTRACT UL
--	---	--	---

SMART ARMOR CONCEPTUAL DESIGN

ABSTRACT

This Final Report is a summary of an eight months effort to determine the feasibility of concepts to design a responsive, resilient armor. Unique materials, armor systems and applications of new technologies to smart armors capable of enhanced ballistic protection and self-healing have been conceptualized and studied to establish feasibility. The promise for such concepts appears excellent, but much work remains to establish the optimum designs and develop them into usable armor systems.

The concepts explored range from passive systems in which unique (to armor) materials properties, such as solid-liquid phase transformations, would be used to maximize energy dissipation; to active concepts, in which micromotors would be used to modify the stress distribution in a favorable fashion, leading to enhanced projectile defeat capability; to concepts in which the armor material would assess the level of damage inflicted by a ballistic impact, and would then "heal" that damage to provide at least a minimal level of protection against additional attack.

Additional concepts of sensing and actuation are explored and unique applications of these traditional smart material concepts to armor are conceptualized.

Modeling of ballistic impact phenomena has been performed using the Pisces program, and limited results are presented indicating the worth of modifying the interaction between stress waves and material surfaces. This is a critical capability in the context of further work, which will use such modelling extensively to investigate such approaches prior to actual experimentation.

I. SCOPE OF WORK

A number of materials design concepts were investigated to determine the feasibility of developing responsive and resilient materials for application in smart armor. Smart armor material systems are envisioned which would possess the ability to react to a threat in a manner that will minimize damage and then allow the armor to "heal" the damage which has occurred. In contrast to other applications of the concept of smart structures, such as vibration control, flaw detection, and active shape changing, the development of smart armor must consider the effect of energies in the range of 0.008 to 0.7 MJ, a response time measured in microseconds, impact velocities of up to 6 km/s, and cracks propagating at 3 km/s. The following issues must be addressed when considering materials for smart armor applications:

- (1) The armor system must rapidly sense the magnitude and location of the impact. More advanced systems would also determine the type and extent of the damage resulting from the impact.
- (2) Portions of the armor system must provide energy sinks or absorption capability at the expected high rates of impact.
- (3) Crack growth must be arrested or retarded through the use of spontaneously reacting mechanisms or materials.
- (4) The armor system must automatically react or deploy materials which will retard further damage and repair existing damage.
- (5) Following the deployment of local materials to effect initial repairs, sensors will report to a damage control system which will transport additional material to complete the healing of the damaged area.

Damage minimization can be accomplished; passively, through intrinsic material properties which maximize energy absorption and dissipation capability, such as phase transformations or rheological responses; actively, through a mechanical response, such as piezoelectrically induced localized compressive force; or by a combination of the two mechanisms. Damage repair can also be accomplished by passive, active or combined modes. Repair concepts are generally envisioned to use material reactions which produce a phase transformation or material migration which fills voids and cracked regions. Advanced concepts seek to mimic the response of biological tissue to tears and punctures.

II. BACKGROUND

II.1 What Is Smartness?

C. A. Rogers, in summarizing the U.S. Army Research Office Workshop on Smart Materials, Structures, and Mathematical Issues¹ provides the following listing of the common features of smart materials and structures:

- (1) Sensors: They have embedded (or bonded) or intrinsic sensor(s) that recognize and measure the intensity of the stimulus (e.g., stress, strain, thermal, electric, magnetic, chemical, radiation, etc.).
- (2) Actuators: They have embedded or intrinsic actuator(s) to respond to the stimulus.
- (3) Control Mechanism: They control responses to the stimulus according to a predetermined relationship and are also capable of selecting a response if more than one option is available.
- (4) Time and Nature of Response: They have fast response to a stimulus. The system returns to its original state as soon as the stimulus is removed.

Newham and Ruschau² have recently treated the question of "How smart is smart?", reaching the conclusion that there are degrees of smartness which they have differentiated in one sense as "passive smartness" versus "active smartness". They describe a passively smart material as one which has the ability to respond to environmental conditions in a useful manner, and differing from an actively smart material in that the former has no external fields or forces or feedback systems to enhance its behavior. The following listing of attributes is given by the authors to summarize some of the meanings of passive smartness:

- * Selectivity
- * Self-diagnosis
- * Self-tuning
- * Sensitivity
- * Shapeability
- * Self-recovery
- * Simplicity
- * Self-repair
- * Stability and multistability
- * Standby phenomena
- * Survivability
- * Switchability

The authors describe active smartness as the process of sensing a change in the environment, and, using a feedback system,

making a useful response. The inference is that in the case of active smartness the feedback system is likely to be external to the material itself while passive smartness is characterized by a feedback system which is intrinsic.

II.2 Current Applications and Examples

Structures which act to minimize damage, absorb energy, or repair themselves are available for certain applications. The most difficult concept to understand is that of a non-biological material system acting to "heal" itself. The most common examples of this are the commercially available automobile tire repair canisters which are able, under certain conditions, to temporarily plug and reinflate a punctured tire; and liquids which stop minor cooling system and automatic transmission leaks.

Smart materials and structures should soon be common place in aerospace applications. Sensors, such as fiber optics and piezoelectrics, will monitor strain or assess damage to aircraft skins. More complex systems will enable wing panels to adjust their shapes to optimize aerodynamics.

The easiest materials to instrument and otherwise make into smart structures are the polymer reinforced composites which are being extensively used in aerospace applications. These materials are formed and cured at relatively low temperatures and pressures permitting instrumentation and control using fiber optics and low temperature piezoelectrics.

It will be evident that in the context of the discussion above, many (but not all) of the concepts will fall under the definition of passive smartness. It should be kept in mind, however, that one of the attributes of passive smartness listed by Newham and Ruschau was simplicity, an indispensable attribute when one wishes to assure the reliable operation of a concept under conditions of great duress, such as those faced by the protective armor of valuable combat assets.

III. SUMMARY OF MOST IMPORTANT RESULTS

This section is a summary of the most important results in the consideration of the feasibility of developing various concepts for responsive and resilient materials. The section includes order of magnitude determinations relevant to armor applications and discussions pertaining to the development of the following concepts: actuation to preserve the integrity of structures, microactuators, projectile defeat and reacting armor.

III.1 Order of Magnitude Determinations

Order of magnitude calculations were made using the following equations and data which is considered relevant to the feasibility of smart material concepts.

III.1.A Salient Features of the Procedure Employed:

The exponential law for reduction of velocity based on Ya Heau³ has been assumed which reads,

$$\dot{v} = \dot{v}_0 e^{-\rho \eta x} \quad (1)$$

where \dot{v}_0 is the striking velocity
 ρ density of the target material, and
 x thickness of penetration

$$\eta = \frac{k_0 A C_D}{m}$$

where k_0 is a constant,
 A area of cross-section of the projectile
 C_D drag coefficient (0.82)
 m mass of the projectile

$$\text{and } t = \frac{\eta \rho (e^{\eta \rho x} - 1)}{\dot{v}_0} \quad (2)$$

where 't' is the time of interaction.

$$P = \dot{v} \frac{I_t I_p}{(I_t + I_p)} \quad (3)$$

where P is the pressure developed when the particle velocity involved is ' \dot{v} '.

I_t and I_p are impedance of target and projectile material, respectively

$$I = \rho V_s \quad \text{where} \quad \rho \text{ is the density and} \\ V_s \text{ is the shock velocity}$$

Temperatures have been estimated based on the table given in Kinslow⁴.

Table I contains descriptions of various cases considered for calculations: battle tank armor against a long rod projectile, aircraft armor against an anti-aircraft projectile and battle tank armor against a missile.

Tables II, III and IV contain data pertaining to silicon carbide and epoxy which correspond to each of the listed cases 1, 2 and 3.

Table V is a tabulation of the material properties used in the order of magnitude calculations.

The data from the tables was then used to generate the order of magnitude values which were then graphed in Figures III.1.1, III.1.2, and III.1.3.

TABLE I. Description of Various Cases Considered for Calculation

Case Number	Description	TARGET				PROJECTILE			Initial Velocity (m/sec)	K in Eqn. (1)
		Front Material		Sandwich Material		Material	Weight (Kg)	Area of Cross Section (m ²)		
		Material	Thicknesses (m)	Material	Thicknesses (m)					
1	Typical case of battle tank armor against long rod projectile	Steel	0.04 0.08 0.12 0.15	SiC and epoxy	0.1 and 0.2	Tungsten Carbide	5.0	0.7E-3	2000	7.0
2	Typical case of aircraft armor against anti-aircraft projectile	Aluminum	0.02 0.02 0.04	SiC and epoxy	0.02 and 0.04	Tungsten Carbide	0.05	0.078E-3	2000	7.0
3	Typical case of battle tank armor against a missile	Steel	0.04 0.08 0.12 0.15	SiC and epoxy	0.1 and 0.2	Copper	0.05	0.0125E-3	6000	2.35

TABLE II. (for Case 1)

Frontal Steel Plate Thickness (m)	Material Thickness (m)	SiC				EPOXY			
		Velocity (m/sec)	Time (μ sec)	Approx. Pressure (GPa)	Approx. Temp. ($^{\circ}$ K)	Velocity (m/sec)	Time (μ sec)	Approx. Pressure (GPa)	Approx. Temp. ($^{\circ}$ K)
0.04	--	1550	23.0	29.0	510	1560	23.0	4.8	850
	0.1	1200	96.5	22.5	420	1400	91.0	4.3	800
	0.2	930	191.0	17.5	390	1275	165.0	3.9	780
0.08	--	1200	52.0	22.5	420	1200	52.0	3.7	750
	0.1	930	147.0	17.5	390	1095	139.0	3.4	540
	0.2	725	268.0	13.5	350	990	235.0	3.1	520
0.12	--	930	90.0	17.5	390	930	90.0	2.9	490
	0.1	725	212.0	13.5	350	850	202.0	2.6	460
	0.2	565	369.0	10.5	330	770	326.0	2.4	450
0.15	--	770	125.0	14.5	355	770	125.0	2.4	450
	0.1	600	272.0	11.0	335	700	261.0	2.2	440
	0.2	465	461.0	8.5	325	640	410.0	2.0	410

TABLE III. (for Case 2)

Frontal Aluminum Plate Thickness (m)	Material Thickness (m)	SiC				EPOXY			
		Velocity (m/sec)	Time (μ sec)	Approx. Pressure (GPa)	Approx. Temp. ($^{\circ}$ K)	Velocity (m/sec)	Time (μ sec)	Approx. Pressure (GPa)	Approx. Temp. ($^{\circ}$ K)
0.01	--	1550	5.7	29.0	510	1550	5.7	4.8	850
	0.02	880	23.0	16.5	370	1250	20.1	3.8	780
	0.04	500	53.4	9.4	325	1000	38.0	3.1	520
0.02	--	1210	13.0	22.5	420	1210	13.0	3.7	750
	0.02	690	35.0	12.9	340	975	31.5	3.0	510
	0.04	390	74.0	7.3	310	780	54.5	2.4	450
0.04	--	735	34.5	13.7	350	735	34.5	2.3	445
	0.02	420	71.0	7.8	320	590	65.0	1.8	390
	0.04	240	135.5	4.5	300	475	102.5	1.5	350

TABLE IV. (for Case 3)

Frontal Steel Plate Thickness (m)	Material Thickness (m)	SiC					EPOXY				
		Velocity (m/sec)	Time (μ sec)	Approx. Pressure (GPa)	Approx. Temp. ($^{\circ}$ K)	Velocity (m/sec)	Time (μ sec)	Approx. Pressure (GPa)	Approx. Temp. ($^{\circ}$ K)		
0.04	--	5100	7.2	75	N/A	5100	7.2	15	N/A		
	0.1	4340	28.5	63	2500	4790	27.2	14	3000		
	0.2	3700	53.5	54	1900	4500	48.9	13	2750		
0.08	--	4350	15.7	64	2500	4350	15.7	13	2700		
	0.1	3700	40.7	54	1900	4090	39.4	12	2600		
	0.2	3150	69.9	46	1500	3840	64.6	11	2500		
0.12	--	3700	25.7	54	1900	3700	25.7	11	2450		
	0.1	3150	55.0	49	1500	3470	53.6	10	2350		
	0.2	2680	89.5	39	1050	3270	83.2	9.5	2250		
0.15	--	3280	34.3	48	1500	3280	34.3	10	2300		
	0.1	2800	67.3	41	1200	3090	65.7	9	2200		
	0.2	2380	106.1	35	900	2900	99.1	8.5	2150		

TABLE V. Appendix
Material Properties Used

DESCRIPTION	MATERIAL					
	STEEL	ALUMINUM	SiC	EPOXY	TUNGSTEN CARBIDE	COPPER
Density (Kg/m ³)	7.896E3	2.785E3	3.12E3	1.198E3	15.02E3	8.93E3
Sound Speed, C ₀ in V _s = C ₀ + gU _p (m/sec)	4569	5328	8000	2678	4920	3940
Compressibility Coefficient g in V _s + Co + gU _p	1.49	1.338	0.95	1.52	1.339	1.489

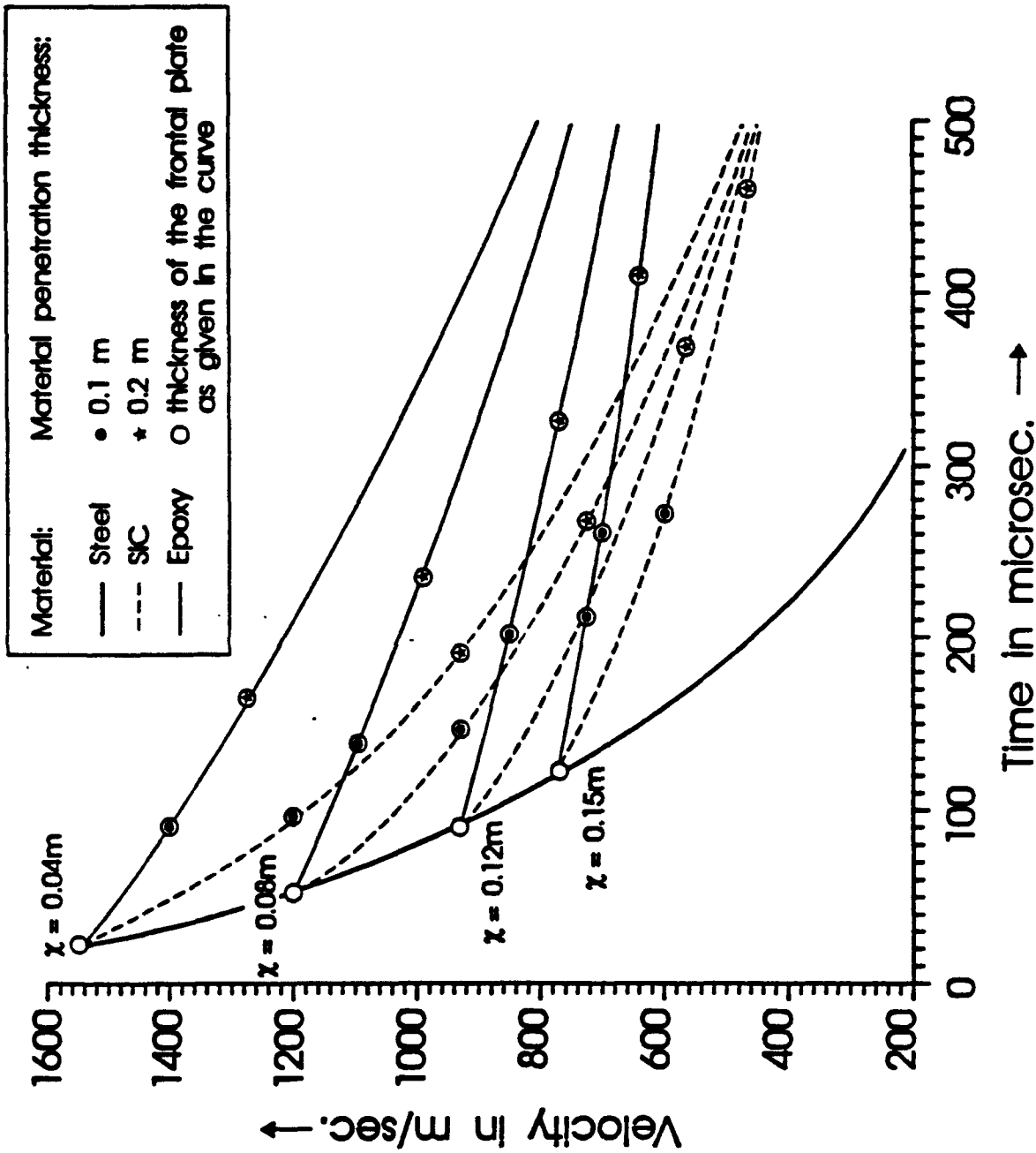


Figure III.1.1.1 Case 1: Battle tank anti tank long rod projectile.

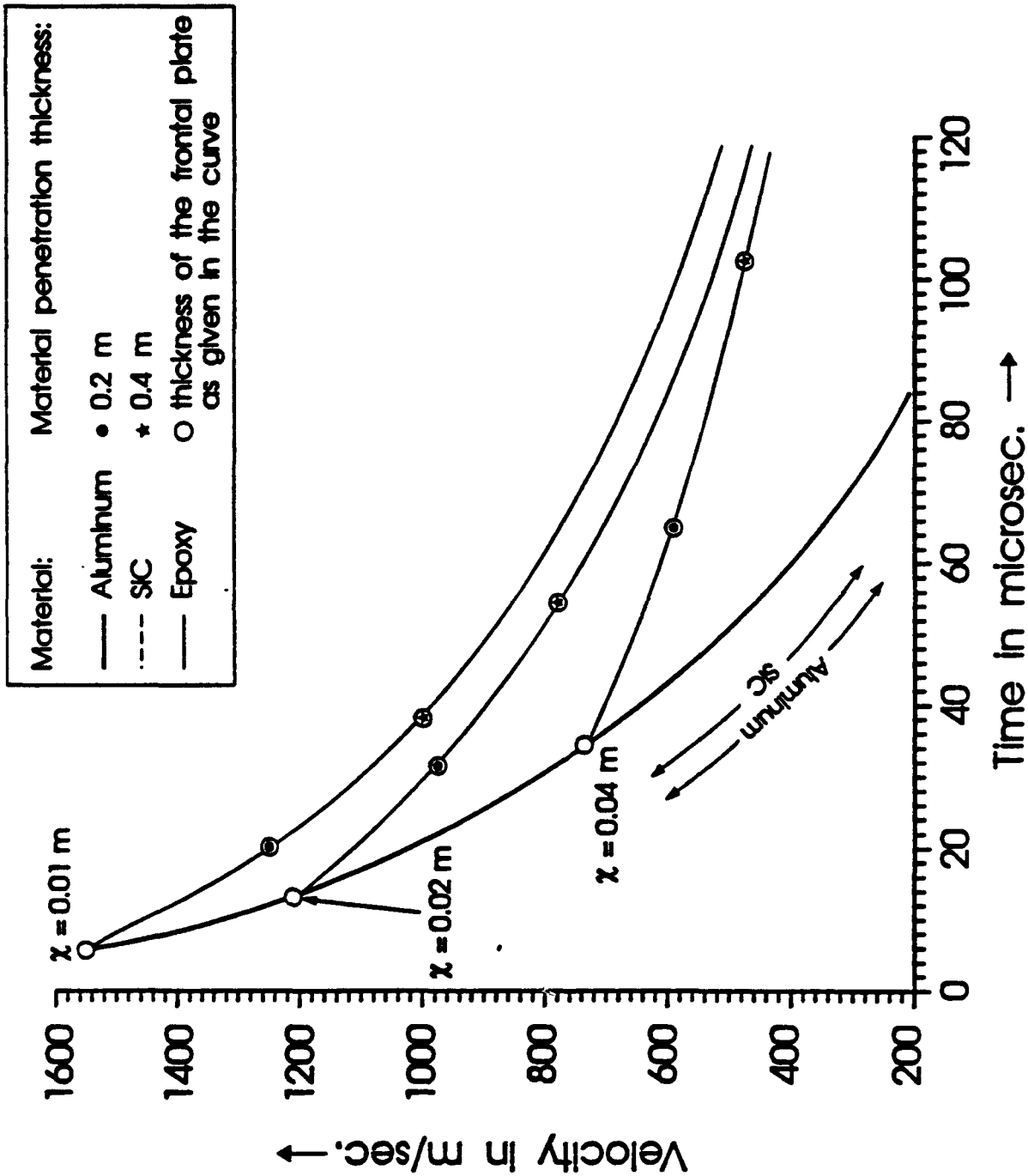


Figure III.1.1.2 Case 2: Aircraft armor against anti aircraft projectile.

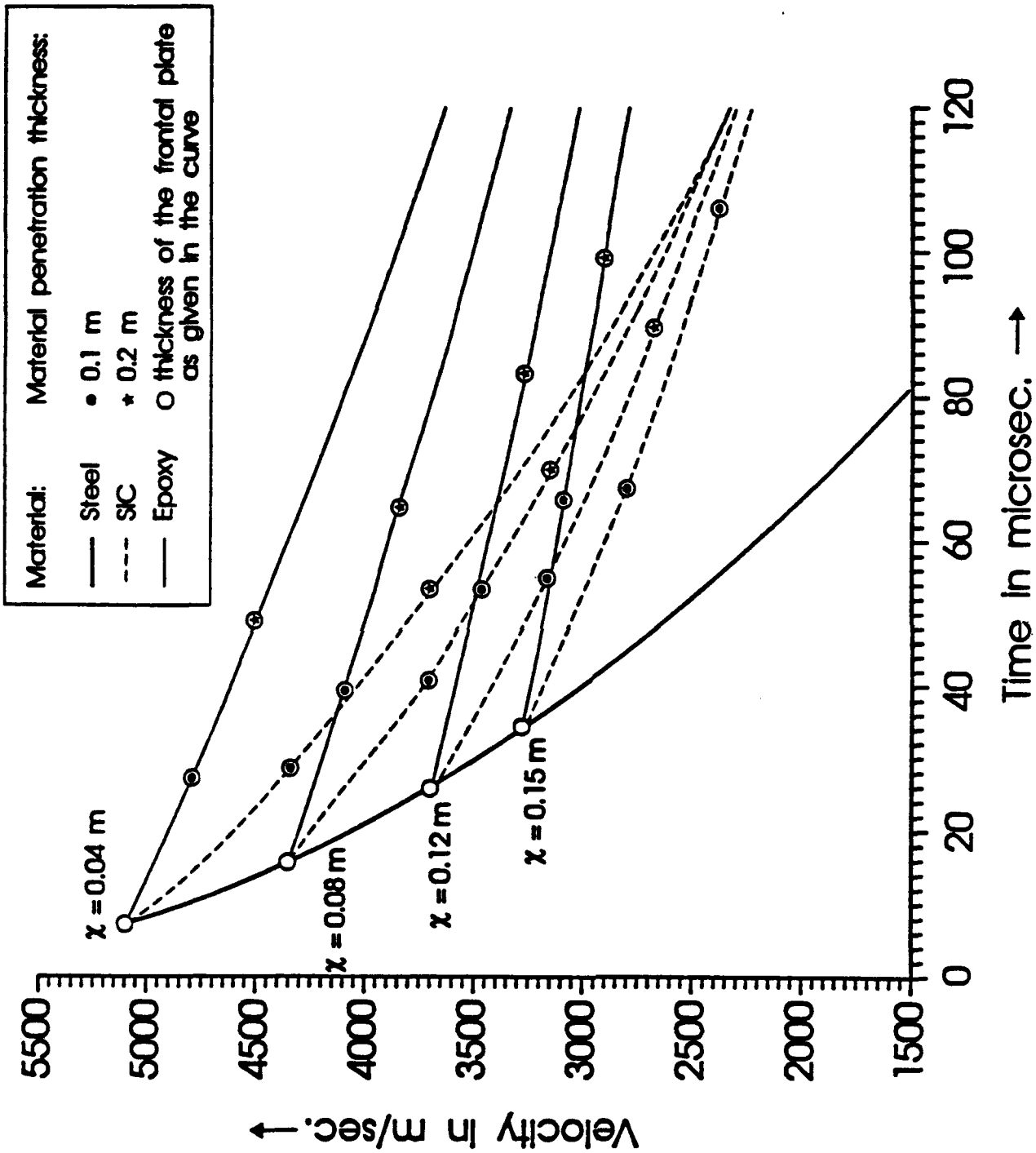


Figure III.1-3 Case 3: Tank/turret armor against missiles.

III.2 Smart Actuation to Preserve Armor Integrity

In this section, we will consider armors that are subjected to high velocity impacts. As a result of the impact, tensile stresses are created away from the impact area. Armor materials do not have sufficiently high tensile strength. As a result, failures including spalling can take place resulting in the armor break-up and a loss of the integrity of the armor. In this section, we are reporting results of our feasibility studies concerning the use of smart actuation to reduce or eliminate these high tensile stresses and to maintain the integrity of the armor structure.

Ground based military vehicles are protected by the use of high strength armor shields. The primary objective of these armor materials is to absorb as much energy as possible from the incoming high velocity projectile so that damage to the structure can be minimized. Typically, materials with extreme hardness and high elastic modulus are preferred for these armor materials. In recent years, there has been a considerable amount of interest in using ceramic based armor materials for military vehicles.

Ceramic materials meet the needs of modern armor systems to withstand high kinetic, thermal or chemical energy levels because of their low density, high elastic modulus and high hardness. But they are brittle and very often exhibit elastic fracture behavior and have much greater compressive strength than tensile strength. The different ceramics that have armor applications are boron carbide, alumina, titanium diboride, silicon carbide, beryllium oxide, silicon nitride and glass-ceramic.

The energy absorption mechanisms in a typical ceramic armor can be explained as follows:

- 1) Initial impact: In this stage, the tip of the projectile is blunted due to the high hardness value of the ceramic tile. This initial impact results in the crushing of the ceramic tile into small pieces thereby absorbing a considerable amount of energy.
- 2) Erosion: In this stage, the blunted round head of the projectile shears through ceramic fragments creating successive layering of fragmented ceramic. During this stage, the target absorbs 60% of the projectile energy.
- 3) Deformation, cracking and fracture: Energy is absorbed in this stage due to failure of the ceramic.

The remaining energy, that is not absorbed, is transmitted to the main structure of the vehicle in the form of a transmitted stress wave. Some of the energy is reflected back to the armor as stress waves. Reflections may create tensile stresses in the

ceramic armor. Since ceramic materials have very poor tensile strength, the development of tensile stresses may result in disintegration of the armor shield thereby making the military vehicle vulnerable to enemy attack. We have examined the feasibility of using smart actuation to reduce or eliminate tensile stresses in the armor.

As a first step, we have developed capabilities for determining induced stresses in a ceramic armor due to the impact of a uranium or steel projectile at velocities exceeding one kilometer per second. Then we studied the development of tensile stresses in the armor target. Following this study, we investigated uses of different types of active restraints that can be imposed to reduce the magnitude of these tensile stresses.

III.2.A High Velocity Impact Induced Stresses

Finite deformation resulting from impact of a high velocity projectile on a brittle ceramic target results in the development of a time dependent stress pattern in the projectile and the target. To determine these stresses and deformations, a software program called MSc-Pisces has been used. This software uses a finite difference scheme.

III.2.B Equations of Motion

The governing Lagrangian equations of motion⁵ are given below for the case of plane strain and axisymmetric conditions. The partial differential equations describing the momentum conservation in an x - y plane are given by

Plane strain conditions:

$$\rho \dot{x} = \frac{\partial \tau_{xx}}{\partial x} + \frac{\partial \tau_{xy}}{\partial y} \quad (5)$$

$$\rho \dot{y} = \frac{\partial \tau_{xy}}{\partial x} + \frac{\partial \tau_{yy}}{\partial y} \quad (6)$$

Axial symmetry conditions:

$$\rho \dot{x} = \frac{\partial \tau_{xx}}{\partial x} + \frac{\partial \tau_{xy}}{\partial x} + \frac{\tau_{xy}}{y} \quad (7)$$

$$\rho \dot{y} = \frac{\partial \tau_{xy}}{\partial y} + \frac{\partial \tau_{yy}}{\partial y} + \frac{\tau_{yy} - \tau_{\theta\theta}}{y} \quad (8)$$

ρ is the density. In axisymmetry, the x axis is the axis of symmetry. γ denotes the direction perpendicular to the x-y plane. The stress tensor, σ_{ij} is separated into a hydrostatic pressure, P , and a stress deviatoric tensor, S_{ij} , as

$$\tau_{xx} = -P + S_{xx} \quad (9)$$

$$\tau_{yy} = -P + S_{yy} \quad (10)$$

$$\tau_{xy} = -P + S_{xy} \quad (11)$$

$$\tau_{\theta\theta} = -P + S_{\theta\theta} \quad (12)$$

The strain rates are related to the local velocities (\dot{x} , \dot{y}) by

$$\dot{\epsilon}_{xx} = \frac{\partial \dot{x}}{\partial y} \quad (13)$$

$$\dot{\epsilon}_{yy} = \frac{\partial \dot{y}}{\partial y} \quad (14)$$

$$2\dot{\epsilon}_{xy} = \frac{\partial \dot{x}}{\partial y} + \frac{\partial \dot{y}}{\partial x} \quad (15)$$

Axial symmetric condition:

$$\dot{\epsilon}_{\theta\theta} = \frac{\dot{V}}{V} \quad (16)$$

The relative rate of change of volume at a point in the material is related to the strain rates by

$$\frac{\dot{V}}{V} = \dot{\epsilon}_{xx} + \dot{\epsilon}_{yy} + \dot{\epsilon}_{\theta\theta} \quad (17)$$

The elastic changes in the stress deviators are

$$\dot{S}_{xx} = 2G \left[\dot{\epsilon}_{xx} - \left(\frac{\dot{V}}{3V} \right) \right] \quad (18)$$

$$\dot{S}_{yy} = 2G \left[\dot{\epsilon}_{yy} - \left(\frac{\dot{V}}{3V} \right) \right] \quad (19)$$

$$\dot{S}_{xy} = 2G \dot{\epsilon}_{xy} \quad (20)$$

Axial symmetric condition:

$$\dot{S}_{\theta\theta} = 2G \left[\dot{\epsilon}_{\theta\theta} - \left(\frac{\dot{V}}{3V} \right) \right] \quad (21)$$

where G is the shear modulus. The hydrostatic pressure P is related to density ρ and specific internal energy e , through an equation of state

$$P = f(\rho, e) \quad (22)$$

The conservation of energy equation can be written as

$$\dot{\epsilon} = \frac{(\tau_{xx}\dot{\epsilon}_{xx} + \tau_{yy}\dot{\epsilon}_{yy} + 2\tau_{xy}\dot{\epsilon}_{xy} + \tau_{\theta\theta}\dot{\epsilon}_{\theta\theta})}{\rho} \quad (23)$$

In the MSc-Pisces code, these equations are programmed to be solved using a finite difference scheme.

In our work, the objective is to investigate terminal ballistics. The governing equations are programmed in Pisces-2DELK. The flow chart for running Pisces-2DELK and its post processor are shown in Figure III.2.1. By using this software, we studied the impact of a uranium projectile on a ceramic armor. The grid pattern used to model the projectile and the armor is shown in Figure III.2.2. In one of the numerical studies, the armor considered has a radius of 100 cms. The projectile is two centimeters in radius X five centimeters in length. Both projectile and target (ceramic armor) are modeled using axisymmetric Lagrange subgrids. Various velocities of the projectile, up to 2000 m/s have been studied. In a second study, grids with sizes of the order of micrometers are considered.

In Figures III.2.3 to III.2.6, plots of distortion of cells in the grid and penetration of the projectile at different times and cycles using the axisymmetric assumption are shown. The contour plot of stresses at the 800th cycle is shown in Figure III.2.7. From these stress contours, it can be observed that the lower portion of armor is completely subjected to tensile stresses.

III.2.C Smart actuation to reduce tensile stresses

Smart actuation is now used to reduce these high tensile stresses developed in the target armor. To study the feasibility, we considered many actuation mechanisms.

I) Complete support of lower portion of armor.

The stress pattern when the lower portion of armor is completely supported is shown in Figure III.2.8. It can be seen that there is a complete shift in the pattern of tensile stresses. By actively changing the support conditions at the lower end of the armor plate, the stress pattern can be changed.

II) Usage of constraint of velocities for different locations.

A mechanism of constraining velocities at specific locations inside the target is considered. This essentially means that the actuation forces must be such that the motion or movement of grid points is restrained by different amounts. Providing this option by using Pisces code is very easy as it is possible to directly constrain the velocity. Figures III.2.9 to III.2.14 refer to control of tensile stresses at the 100th cycle by using an active control to restrain movement of certain grid points. The tensile

stress contour plots when different zone points are constrained at the 800th cycle are shown in Figures III.2.15 and III.2.16. The dark lines in all figures indicate the locations where the velocities are constrained.

If we re-examine the results at the microlevel, each of the $1 \times 1 \times 1 \mu^3$ subgrids is subjected to a momentum of 5×10^{-12} kg-m/sec. To constrain the velocity the subgrid should be subjected to a momentum of -5×10^{-12} kg-m/sec. This amount of momentum can be developed by microactuators or micromotors embedded in the ceramic armor. These micromotors are of miniature size and can generate force and torque. The available micromotors and their capabilities are discussed in the next section.

From the above study it can be concluded that it is possible to identify and eliminate tensile stresses completely or reduce them to a desired level by using smart actuation.

III.2.D Smart actuators

Our feasibility study has indicated that by providing active restraints inside the armor and at the boundaries, we can control tensile stresses and preserve the integrity of the armor. Next, we have to explore methods of providing the needed actuation, sensing the need for such an actuation and developing techniques to implement active control. Following these studies, we can conduct tests to validate the concept of bonding or embedding the sensors, actuators and active control mechanism.

There are many different ways to implement the required actuation. One of the methods is to embed piezoceramic or ceramic electrostrictive actuators to provide the needed constraints. The second option is to use micromotors to achieve the needed actuation. It is to be noted that both piezoceramic actuators and micromotors are made from ceramic materials. The needed sensing can be achieved by many different techniques including piezoelectric transducers. The projectile impact velocity can be of the order of 1 to 3 kilometers per second. The elastic wave propagation velocity inside the target material is of the order of 13 kilometers per second; therefore, there will be sufficient time to react to the the threat of the penetrating projectile, using fast responding sensors and actuators.

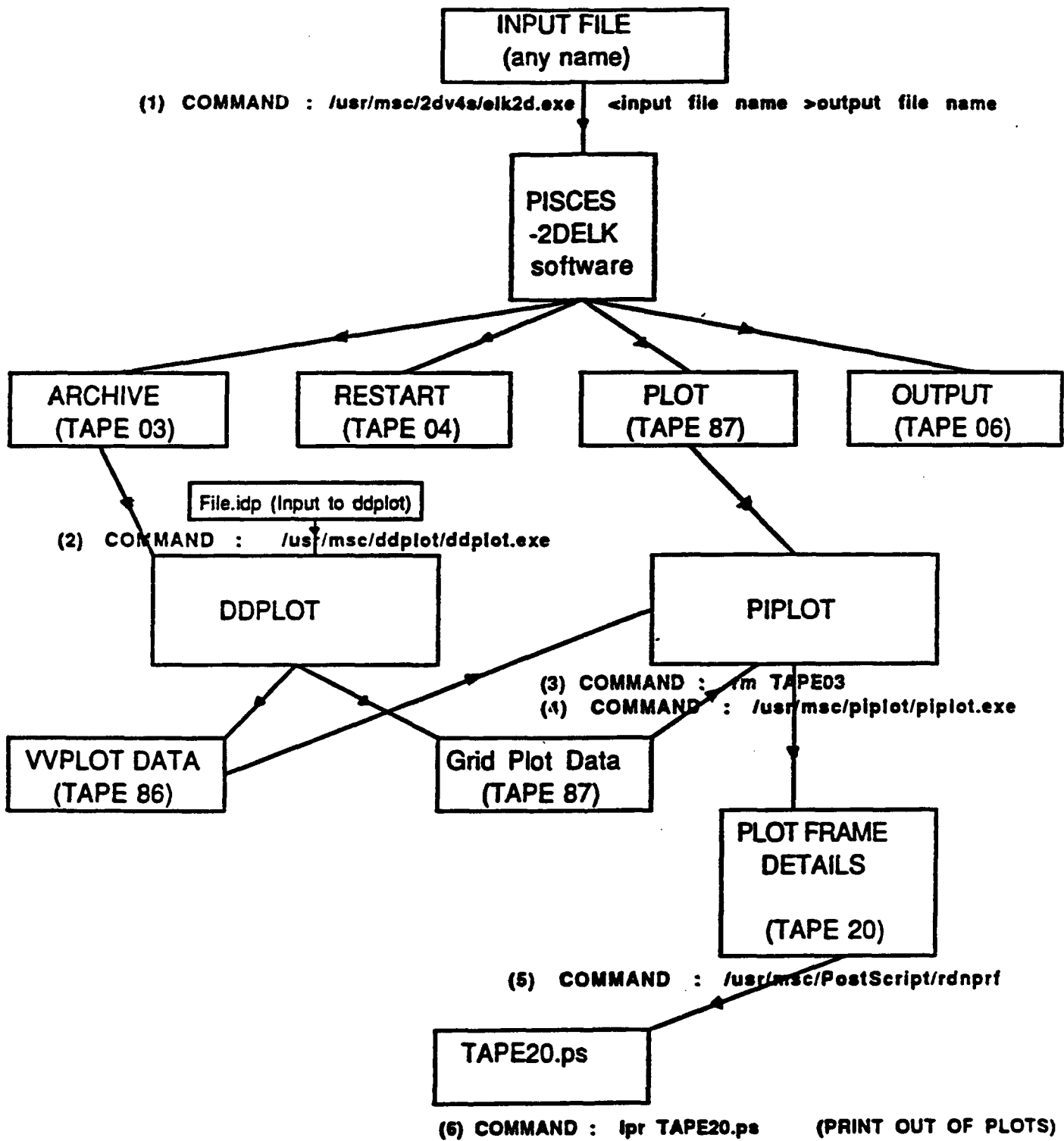


Figure III.2.1 Flow chart for running PISCES-2 DEL K.

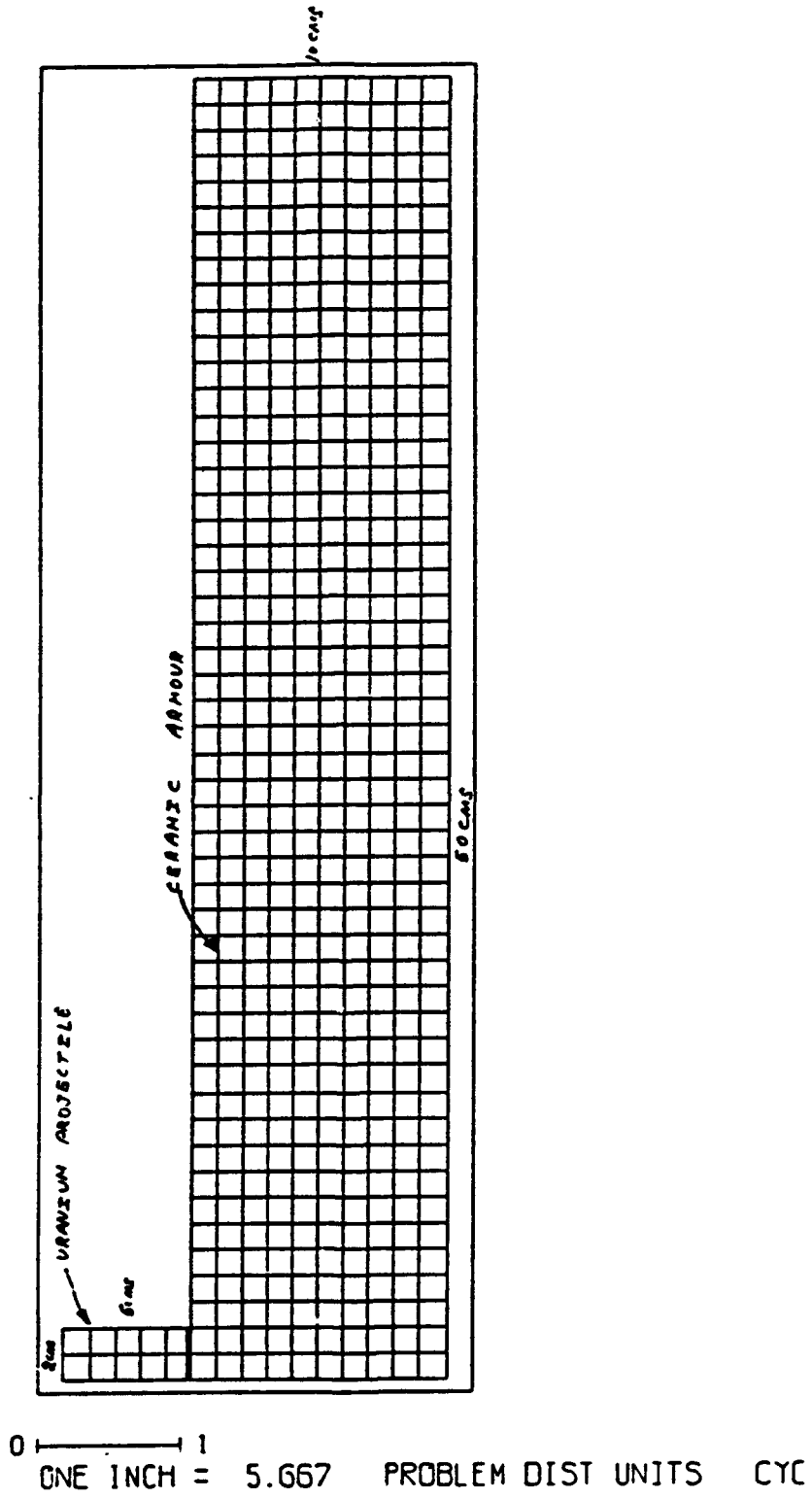
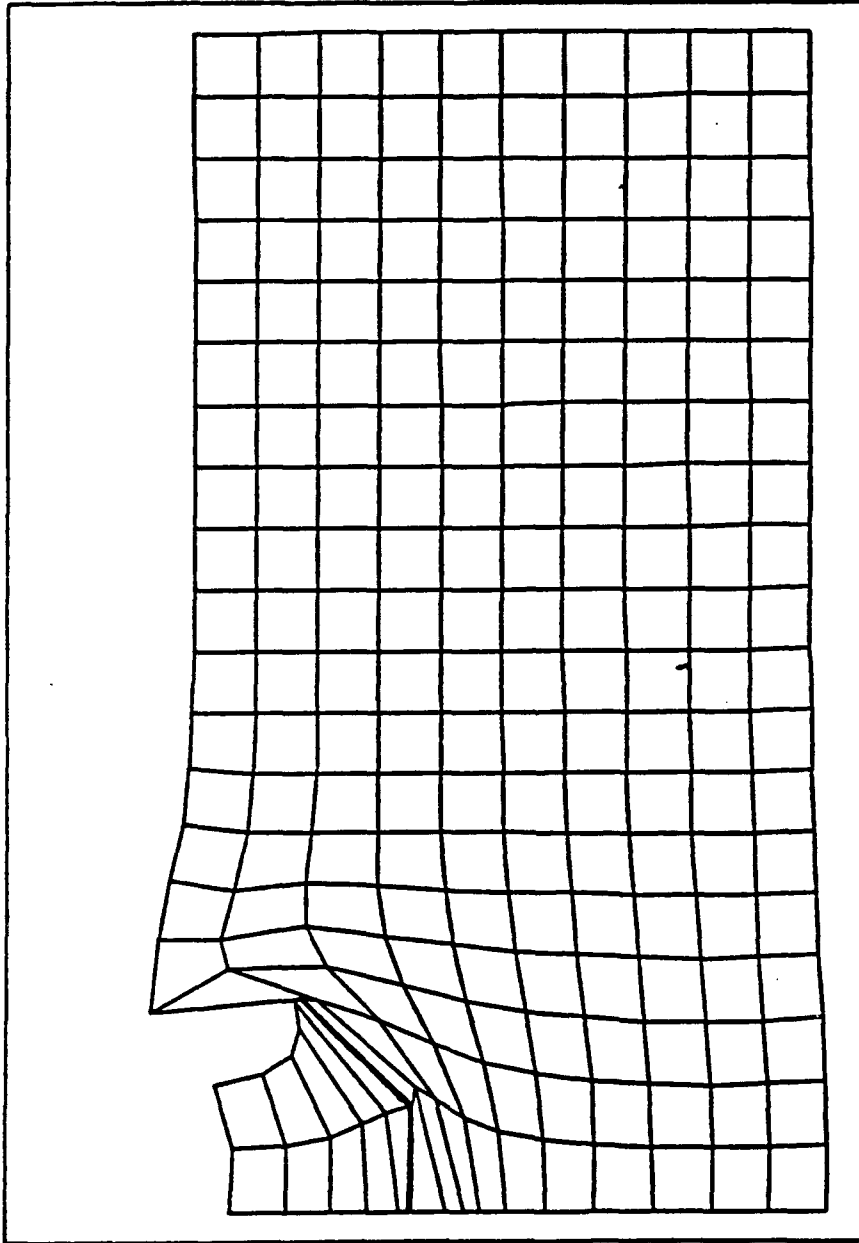
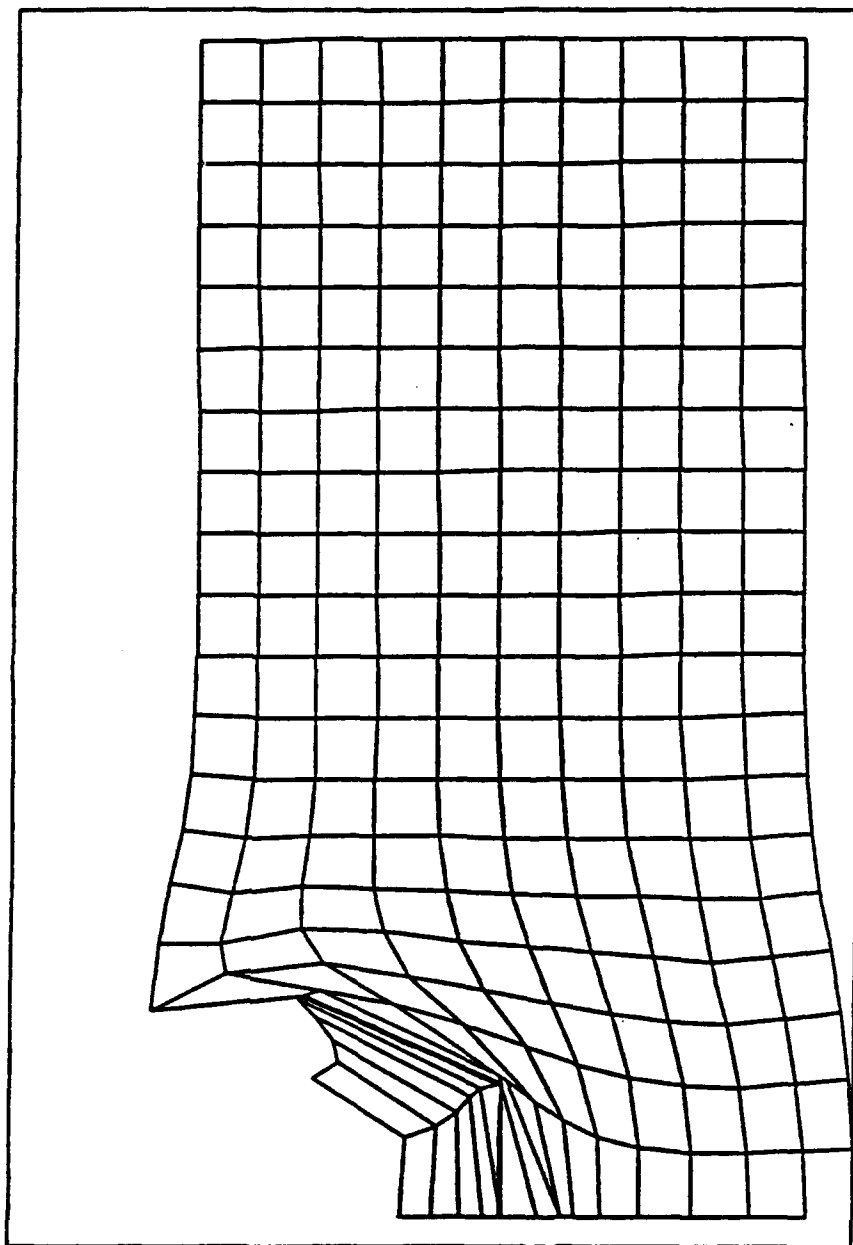


Figure III.2.2 Mesh plot showing grid scheme for projectile and armor.



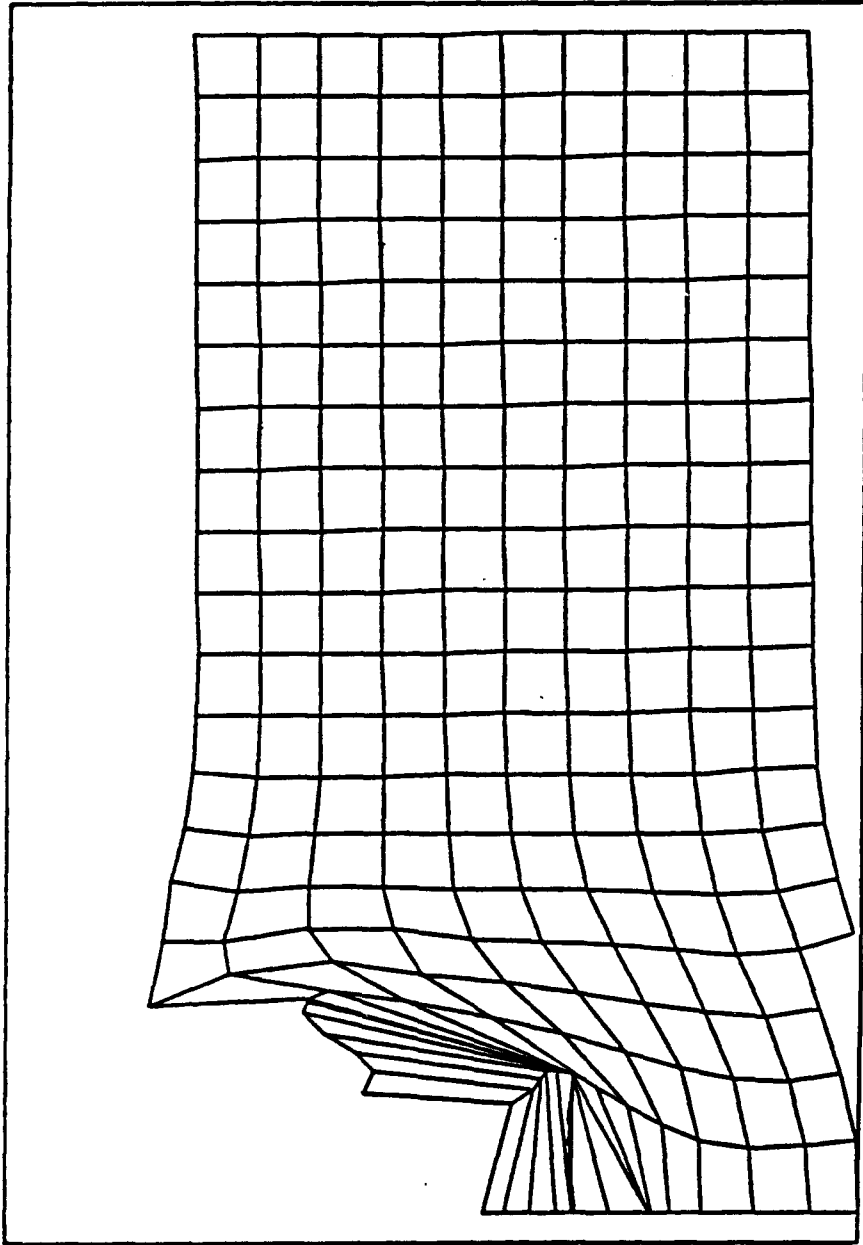
0 ——— 1
ONE INCH = 2.222 PROBLEM DIST UNITS CYCLE 200

Figure III.2.3 Distortion contour after 200 cycles.



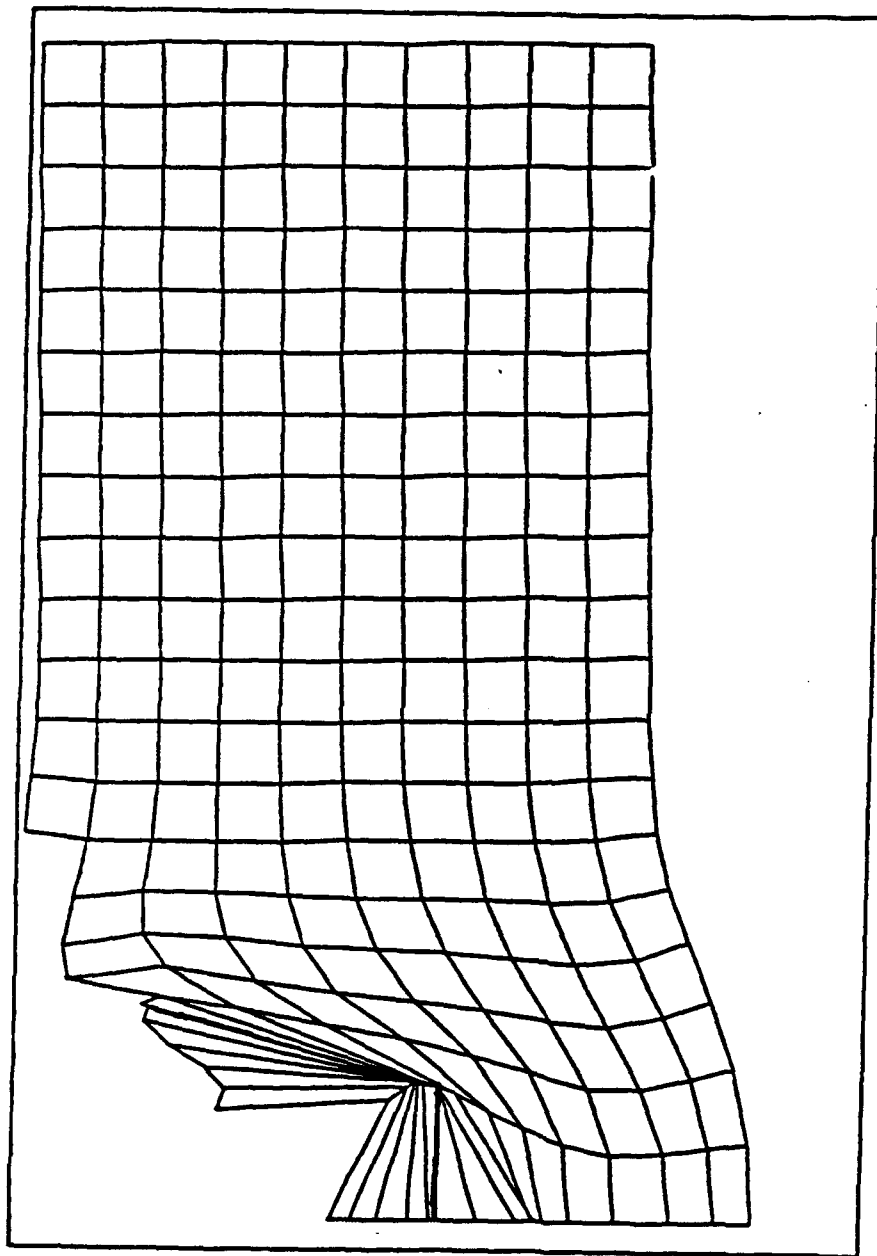
0 ——— 1
ONE INCH = 2.222 PROBLEM DIST UNITS CYCLE 400

Figure III.2.4 Distortion contour after 400 cycles.



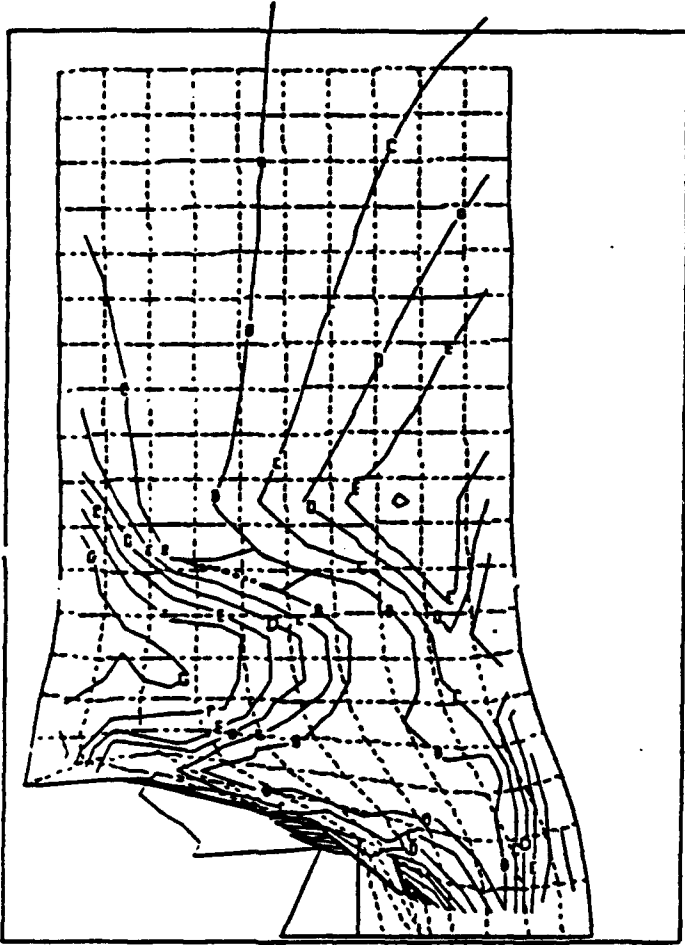
0 ——— 1
ONE INCH = 2.222 PROBLEM DIST UNITS CYCLE 600

Figure III.2.5 Distortion contour after 600 cycles.



0 ——— 1
ONE INCH = 2.222 PROBLEM DIST UNITS CYCLE 800

Figure III.2.6 Distortion contour after 800 cycles.



0 ——— :
 ONE INCH = 2.222 PROBLEM 0157 UNITS CYCLE 800

CONTOUR LEVELS

A	0.0
B	.005
C	.01
D	.015
E	.02
F	.025
G	.03
H	.035
I	.04
J	.045
K	.05

Figure III.2.7 Stress contour after 800 cycles.

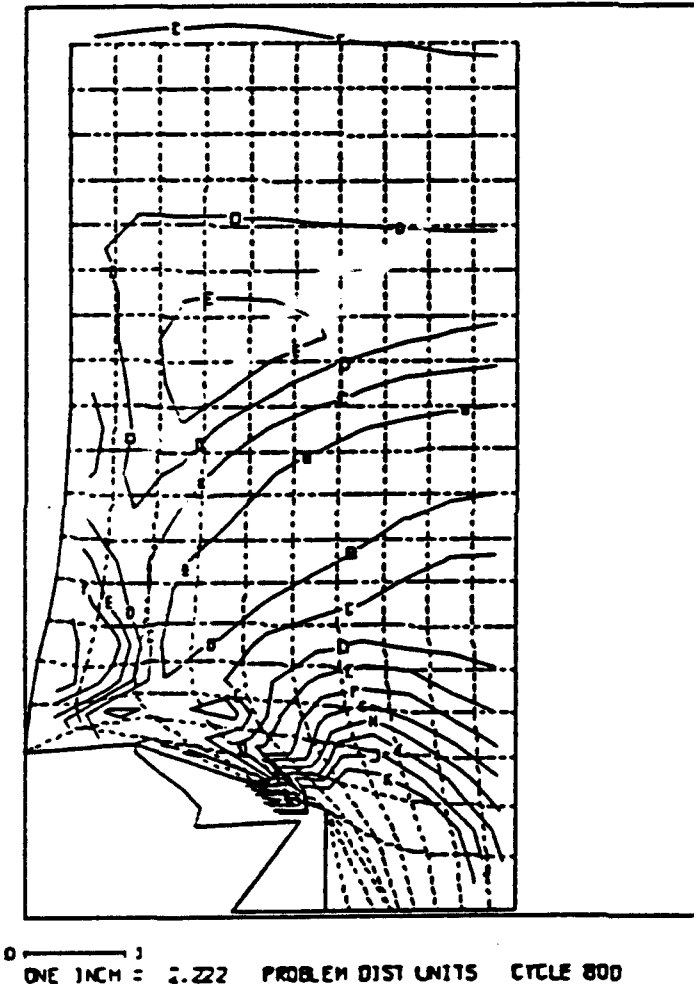
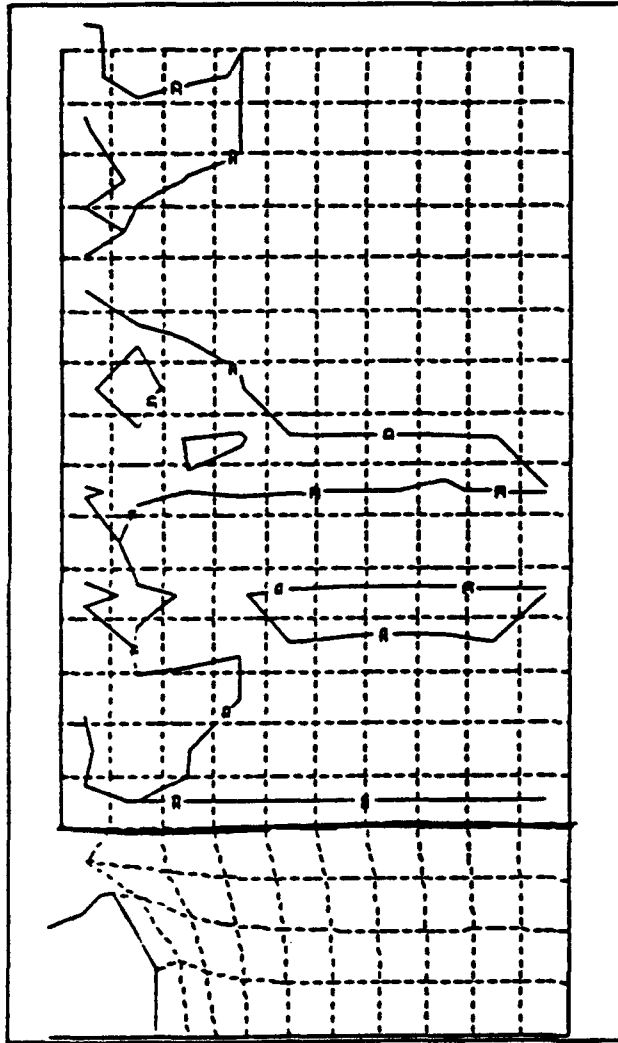


Figure III.2.8 Stress contour after 800 cycles with lower portion of the armor supported.

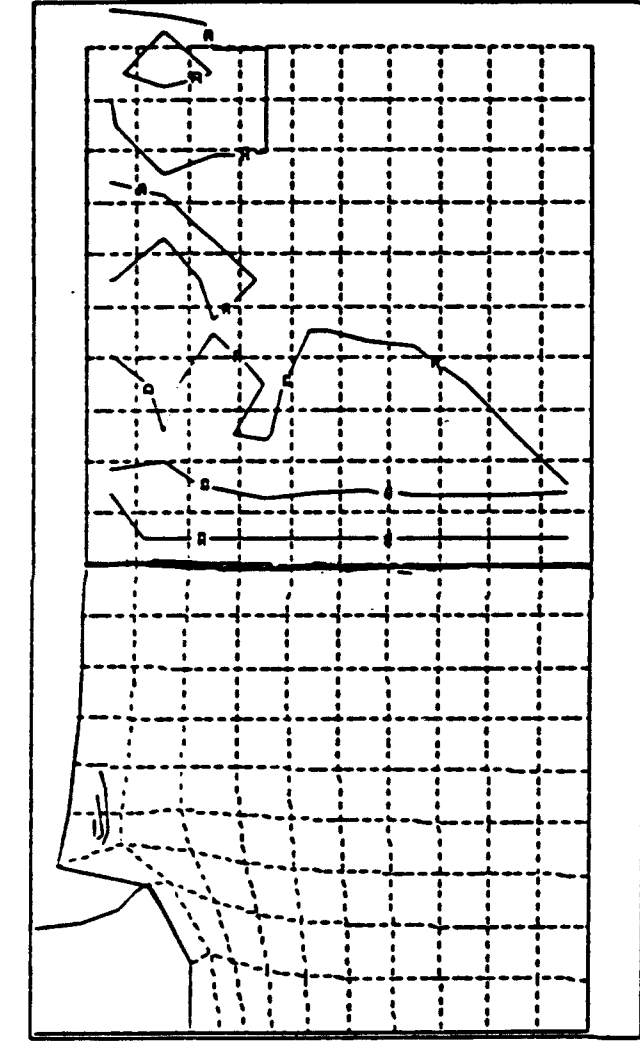


CONTOUR LEVELS

A	0.0
B	.005
C	.01
D	.015
E	.02
F	.025
G	.03
H	.035
I	.04
J	.045
K	.05

 :
 ONE INCH = 2.222 PROBLEM DIST UNITS CYCLE 100

Figure III.2.9 Stress contour after 100 cycles with smart actuation.

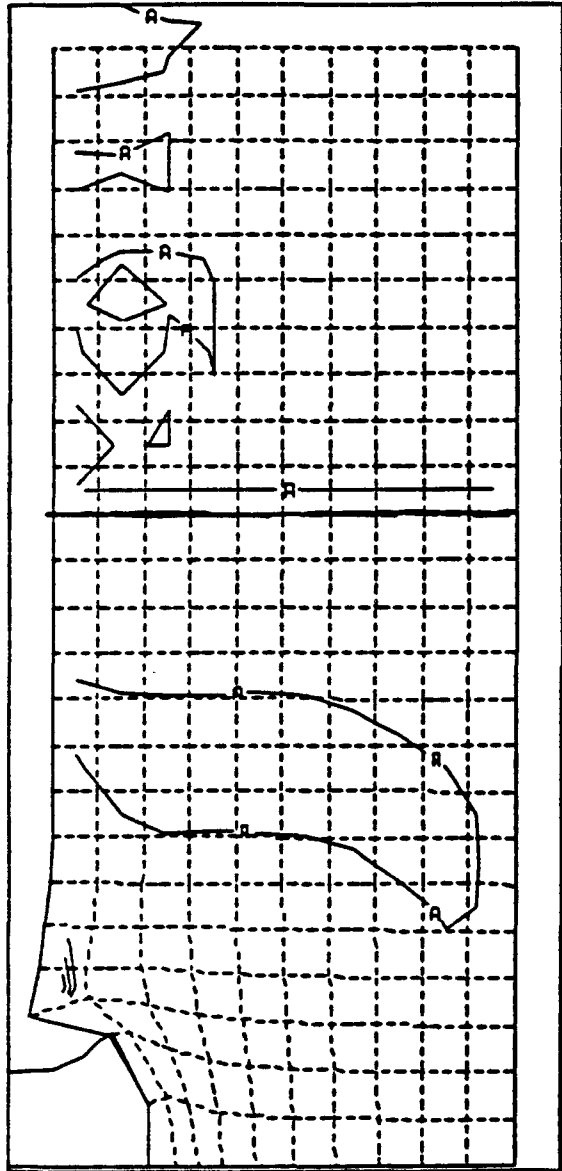


CONTOUR LEVELS

A	0.0
B	.005
C	.01
D	.015
E	.02
F	.025
G	.03
H	.035
I	.04
J	.045
K	.05

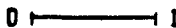
0 ——— :
 ONE INCH = 2.222 PROBLEM DIST UNITS CYCLE 100

Figure III.2.10 Stress contour after 100 cycles with smart actuation.



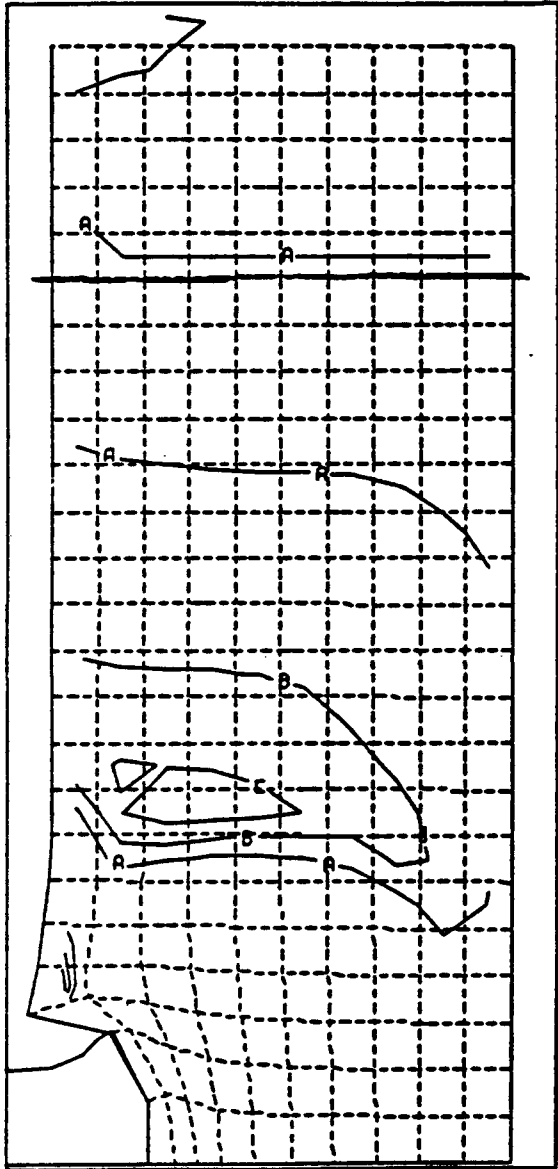
CONTOUR LEVELS

A	0.0
B	.005
C	.01
D	.015
E	.02
F	.025
G	.03
H	.035
I	.04
J	.045
K	.05



 ONE INCH = 2.778 PROBLEM DIST UNITS CYCLE 100

Figure III.2.11 Stress contour after 100 cycles with smart actuation.

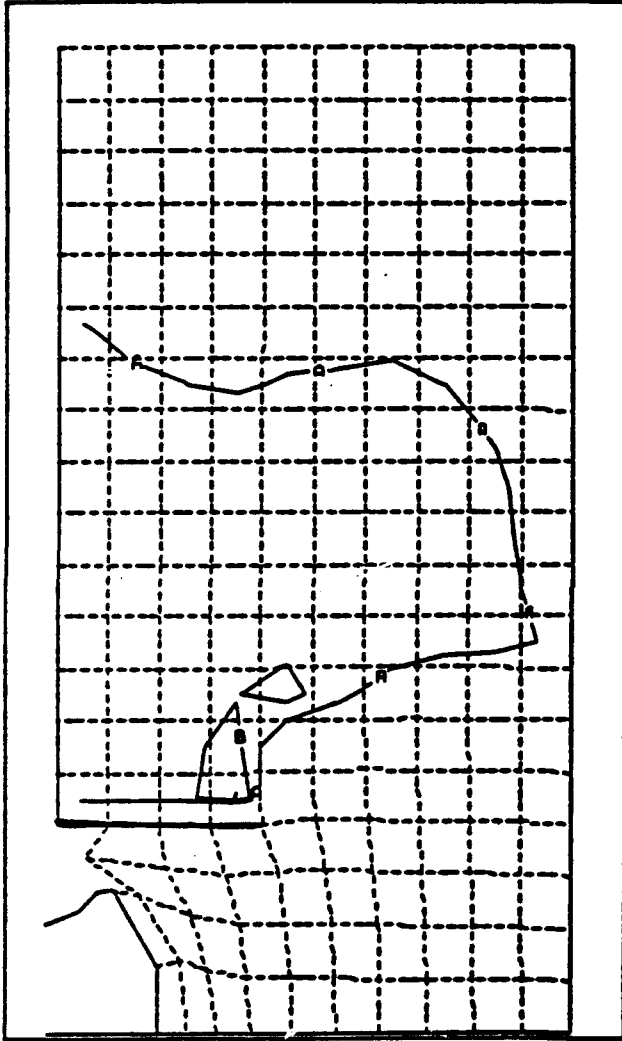


CONTOUR LEVELS

A	0.0
B	.005
C	.01
D	.015
E	.02
F	.025
G	.03
H	.035
I	.04
J	.045
K	.05


 ONE INCH = 2.778 PROBLEM DIST UNITS CYCLE 100

Figure III.2.12 Stress contour after 100 cycles with smart actuation.

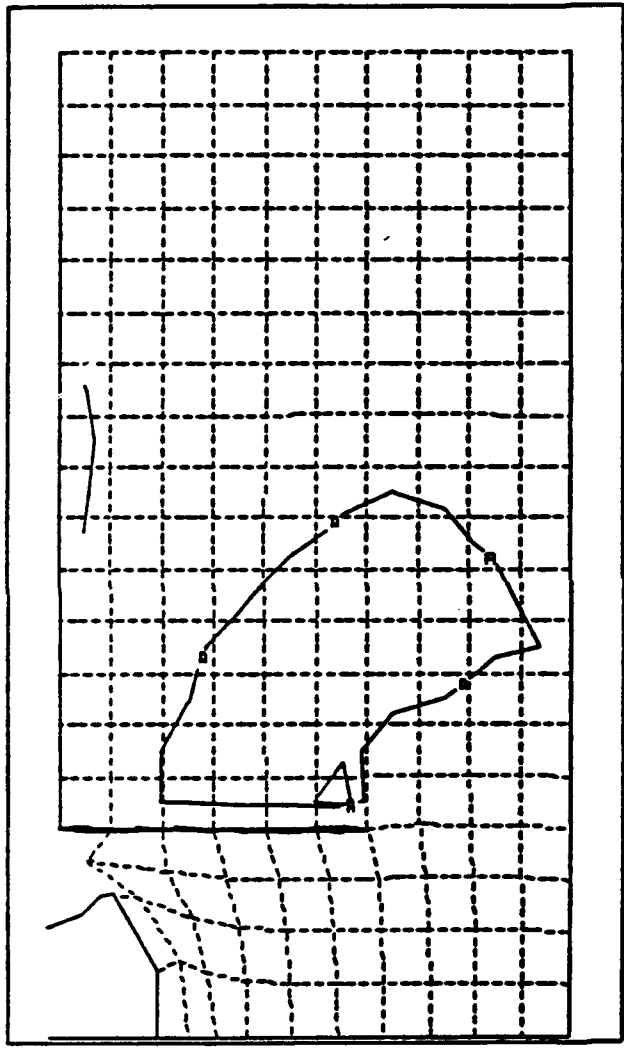


CONTOUR LEVELS

A	0.0
B	.005
C	.01
D	.015
E	.02
F	.025
G	.03
H	.035
I	.04
J	.045
K	.05

0 ——— 1
 ONE INCH = 2.222 PROBLEM DIST UNITS CYCLE 100

Figure III.2.13 Stress contour after 100 cycles with smart actuation.

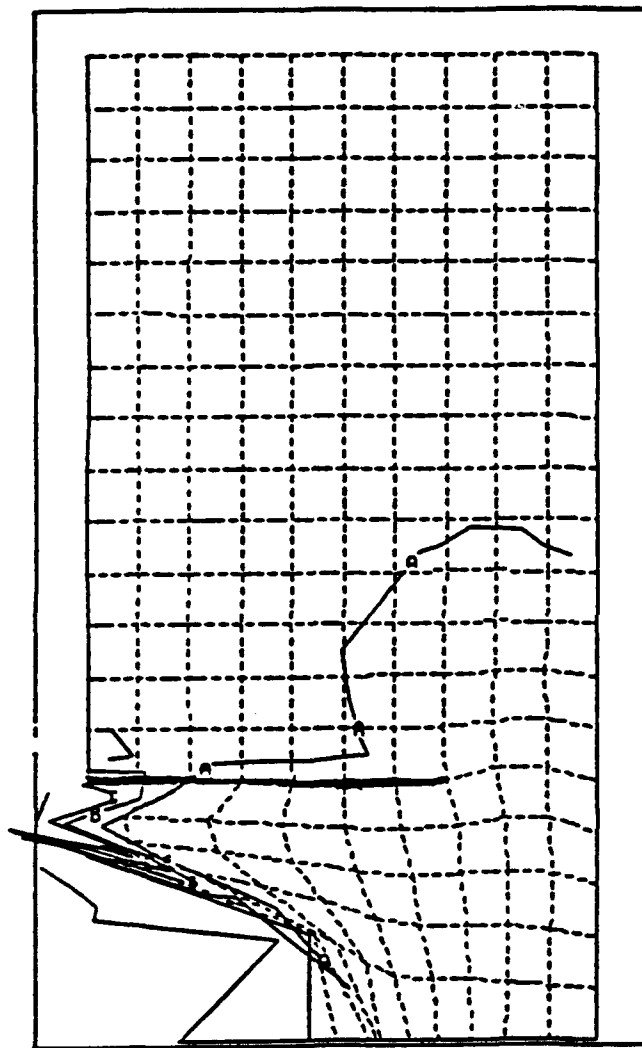


CONTOUR LEVELS

A	0.0
B	.005
C	.01
D	.015
E	.02
F	.025
G	.03
H	.035
I	.04
L	.045
M	.05

0 ——— 1
 ONE INCH = 2.222 PROBLEM DIST UNITS CYCLE 100

Figure III.2.14 Stress contour after 100 cycles with smart actuation.

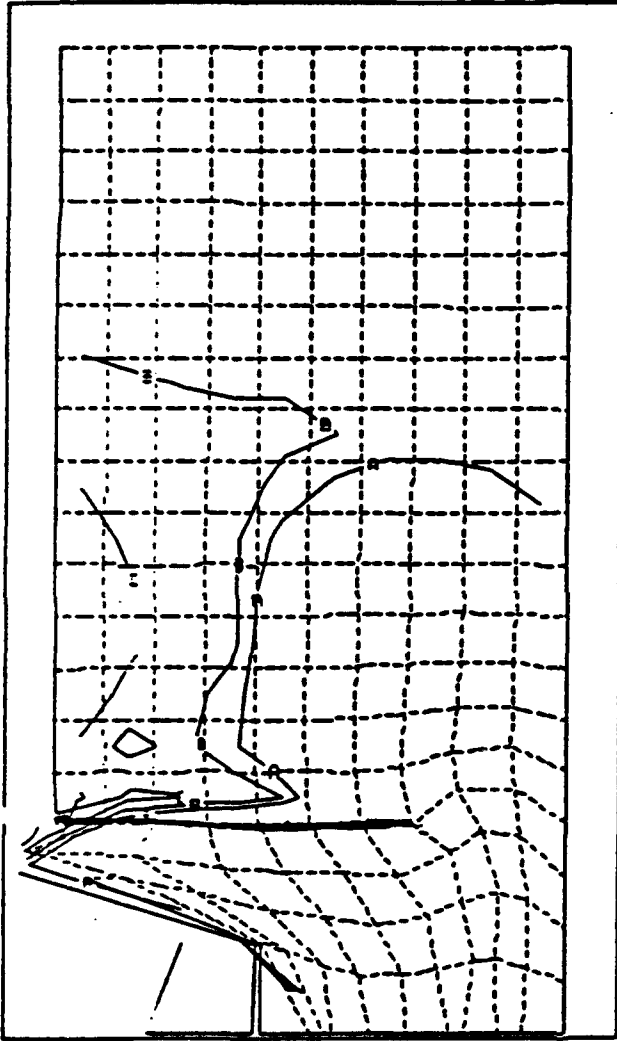


CONTOUR LEVELS

A	0.0
B	.005
C	.01
D	.015
E	.02
F	.025
G	.03
H	.035
I	.04
L	.045
K	.05

0 ——— 1
 ONE INCH = 2.222 PROBLEM DIST UNITS CYCLE 800

Figure III.2.15 Stress contour after 800 cycles with smart actuation.



CONTOUR LEVELS

A	0.0
B	.005
C	.01
D	.015
E	.02
F	.025
G	.03
H	.035
I	.04
L	.045
K	.05


 ONE INC- = 2.222 PROBLEM DIST UNITS CYCLE 800

Figure III.2.16 Stress contour after 800 cycles with smart actuation.

III.3 Microactuators and their Application to Smart Armors

The objective of the study is to explore the feasibility of using micromotors to change the constitutive equations of a material. The objective may be achieved by making the micromotors (with dimensions of 10-50 microns or smaller as the technology becomes available) an integral part of the armor material. By properly orienting these micromotors, and selecting appropriate power input, we would propose to induce a specific change in the deformation of the structure. This change can be very different from the deformations expected under a given loading. Such changes can be used either to provide internal restraints to eliminate tensile stresses in the target or to change the direction of the momentum of the impacting projectile. In the first section, a brief background of micromotors, their working principles and their capabilities are reviewed.

III.3.A Micromotors

Actuators of miniature size are called micromotors. Currently, micromotors are used in many areas where handling of small parts is involved. One of the motivations for these applications is based on the fact that smaller systems can move small parts much faster and more effectively than large systems. In addition, thermal expansion and vibration problems are minimal when small systems are used. It is easier to obtain high accuracy with small systems and because the floor space required is minimal, they can be incorporated at intricate locations without much difficulty.

Electric motors that employ electromagnetic forces are normally used in large scale systems. However, scaling down the size of electromagnetic motors results in a rapid decrease in the amount of generated mechanical power. This makes electromagnetic motors less suitable for our applications. However, motors that work on electrostatic principle can provide appreciable amount of power at microlevels⁶.

Electrostatic motors are electric motors that create mechanical motion using electrostatic forces. The invention of the electrostatic motor is attributed to Gordon (1742). Gordon made an electric bell that used electrostatic forces. In 1752, Franklin used such bells to design a warning system that started ringing whenever the rod connected to the electric bells was electrified. Behrens developed an electrical pendulum in 1806 and Daily developed a reciprocating motor in 1880. Despite the long history, at the macrolevel, electrostatic motors were not popular in practice because they required high voltages and it was difficult to achieve high mechanical accuracy. However, their capability to generate considerable amount of mechanical power at microlevels, the advent of silicon technology, and the development of advanced micromachining capabilities has led to wide usage of electrostatic motors as micromotors.

III.3.B Principle of Micromotors

Micromotors operate at the micro level. Most of the available micromotors are electrostatic motors. "Electrostatics is a phenomenon of interaction of electrical charges that depends solely on the relative position of charges" and does not depend on relative motion.⁷ If two plates of a parallel plate capacitor are slightly displaced with respect to each other, an electrostatic force that has a tendency to realign the plates is developed parallel to the plates. These motors convert electrical forces into mechanical forces. Depending on the way these forces are delivered to the motor, the micromotors can be subdivided into contact motors, spark motors, corona motors, or induction motors. Depending on the operational mode of the motor, they can be subclassified as dielectric micromotors or capacitor micromotors. Depending on the rate of rotation relative to the period of applied voltage, these motors can also be classified as synchronous or asynchronous motors.

Micromotors can also be developed using smart materials such as piezoelectric materials, electrostrictive materials and shape memory alloys. The basic principle involved in these cases is that by the application of an electric field (or a thermal field), a force will be generated which can then be used to do mechanical work. Currently available micromotors and their capabilities are discussed in the next section.

III.3.C Available Micromotors

During the past few years (since 1987) a significant amount of research has been done in the area of micromotors.^{8,9,10,11,12,13,14,15,16,17,18,19,20} The focus of research is to reduce their size and to find new applications of these miniaturized motors. In 1987, Trimmer and Gabriel of AT&T Laboratories²¹ discussed the design considerations of electrostatic micromotors. They designed linear and rotary electrostatic motors. They showed that at 100 volts, linear electrostatic motors of five centimeters in length and one micrometer width could generate a force of 1.87 Newtons. Rotary electrostatic motors with a one millimeter radius rotor can generate a force of 1.4 Newtons.

Fan, Tai, and Muller²² at Berkely Sensor and Actuator Center have developed electrostatic force driven micromotors that have been manufactured using integrated circuit processing. The stator and the rotor were made from 1.5 microns thick polycrystalline silicon. The diameters of the rotors used in their motors were on the order of 60 to 120 microns. Using 350 volts, an angular velocity as high as 500 rpm was achieved (Figure III.3.1).

Fujimoto, Sakata et.al.²³ of OMRON corporation, Japan have developed a miniature electrostatic motor with a 5.5 millimeter

rotor diameter. The torque generated by the motor could not be measured by the conventional motor torque meters because of the extreme small sizes involved. Because of this, torque was measured through special procedures involving the frictional resistance of the pivot bearings. At 600 volts, they generated a torque of 2.5×10^{-4} gf cm. The rotor and stator were made of brass.

Tai and Muller²⁴ of Berkely Sensor and Actuator Center have fabricated electrostatic synchronous micromotors using techniques derived from integrated circuit micro circuit fabrication techniques. They were able to drive their micromotors at considerable angular velocities using voltages on the order of 100 volts. Typical dimensions of the rotors used in these motors were in the range of 120 micrometers. The details of the fabrication process of these motors are as follows. A typical motor consists of a stator, a rotor and a motor hub that holds the rotor. Initially, the micromotor is built on a composite layer composed of 300 nm of silicon dioxide and one millimeter of silicon nitride. This layer helps to prevent electrical breakdown between the motor and the silicon substrate. This latter layer also protects the silicon dioxide layer from dissolving when the sacrificial layer is dissolved. After this layer is formed, these layers are covered with a 2.2 millimeter thick layer of phosphosilicate glass which acts as the sacrificial layer. A polysilicon layer of 1.5 millimeters is deposited and oxidized to have a 100 nanometer thermal oxide on the top. The polysilicon-oxide composite layer is then plasma etched to form the rotor and stators. The sacrificial layers are then removed by using an appropriate etchant. (Figure III.3.2)

Kuribayashi²⁵ of University of Osaka has developed a millimeter sized motor made of shape memory alloy. He used this micromotor as a miniature robot to assemble small mechanical parts. Research is underway to reduce the size of the motor. A phase change in the constrained shape memory alloy with the application of temperature is responsible for the actuation force. With this micromotor, Kuribayashi was able to generate a force of one kgf by increasing the temperature to 85°F. The main drawback of using the shape memory alloy is its poor response time. However, the smaller alloy is faster in response (Figure III.3.3).

Higuchi, Yamagata, Furutani and Kudoh²⁶ of Tokyo University used electrostrictive stacks for microactuation. They were able to generate a force of 10 kgf using a stack of 10 mm length and 3 mm thickness with 150 Volts. They used an "impact drive mechanism" to move miniature objects from one place to another. It was possible to position microparticles within an accuracy of one micron. Controlled expansion and contraction of the electrostrictive material constitutes the "impact drive mechanism". A typical impact drive mechanism can be demonstrated using the steps described in Figure III.3.4.

Ultrasonic micromotors ²⁷ that use the power of an acoustic wave have been developed by Moroney, White and Howe of the Berkely Sensor and Actuator Center. They used flexural lamb waves to create motion in thin membranes that are supported by silicon dies. Using an acoustic wave of power one mW, they observed motion at voltages as low as 1.5 volts. They were able to produce both linear and rotary motion using lamb waves. These ultrasonic motors may have a special application in the design of smart armor. The impact of a projectile create stress waves. These stress waves can be used to drive micromotors to preserve the structural integrity of the armor or even to defeat or deflect the impacting projectile.

III.3.D Application to the Case of Ceramic Armors

In this section, we are considering the impact of a steel projectile on a ceramic target under plane strain conditions. We will assume that the micromotors are embedded in the target at selected locations. We would like to explore the feasibility of microactuators to change the direction of the momentum of the impacting projectile.

For the purpose of the feasibility study, let us consider an armor plate one meter thick and 10 meters in length. Let us assume that the first 11 centimeters of the frontal edge are embedded with ceramic based micromotors. The frontal edge is considered because that edge represents the impact surface. (Figure III.3.5)

Along the x-axis (Figure III.3.5), 100 micromotors of 0.0001 meters radius placed one next to the other will occupy one centimeter. If they are placed one millimeter apart, the length occupied by the micromotors will be 11 centimeters. Along the y-direction, we can place many more micromotors. Let us assume that we can activate 1000 micromotors along the y-direction. This means, each row will have 1000 micromotors providing 2.4 newtons of force per micrometer. We would like to achieve 1 to 10 meters per second actuation. Then, as the projectile penetrates 11 centimeters in depth along the x-direction, we will have created 100 to 1000 meters per second actuation in the y-direction. This should be sufficient to change the direction of the momentum of the impacting projectile. The effect of the y-direction actuation on the direction of momentum of the incoming projectile in microlevel using MSc-Pisces code has been studied.

A steel projectile with a velocity of 1000 meters per second is made to impact on a ceramic armor. The setup of the model used for the analysis is shown in Figure III.3.6. The eight cells marked in the armor are given an x-direction actuation of 1000 meters per second at the end of the first cycle and the results are recorded at the end of the third cycle. The bullet momentum in the x and y directions was observed to be $7.895e^{-16}$ kg-m/sec and $2.887e^{-20}$

kg-m/sec respectively. The angle of deviation of the bullet is observed to be $2.096e^{-3}$ degrees. Distortion plots of the bullet for the first 10 cycles are shown in Figures III.3.7-III.3.10. Hence, it can be noted that it is possible to change the direction of the momentum of the bullet using microactuation.

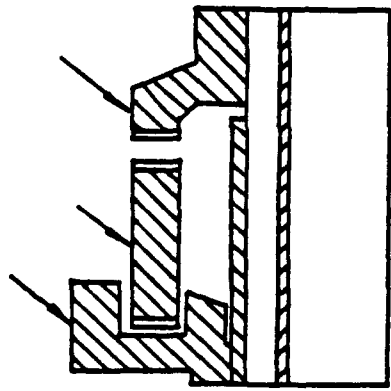


Figure III.3.1 A schematic of an electrostatic micromotor.

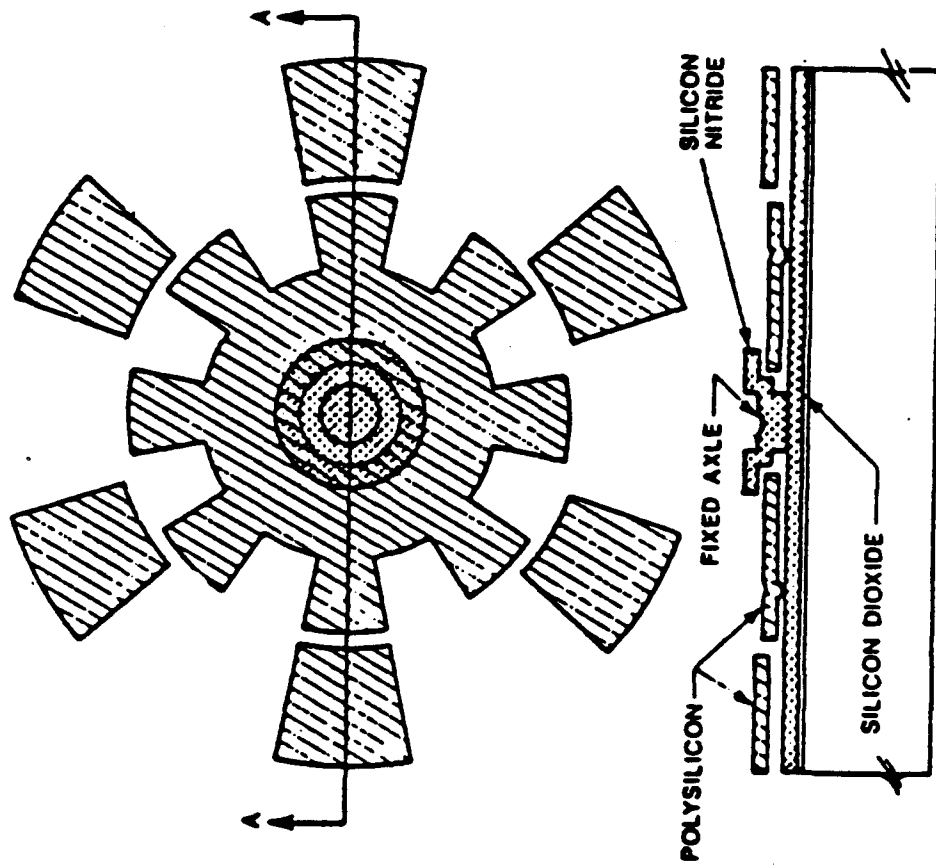


Figure III.3.2 Top and cross-sectional views of a micromotor.

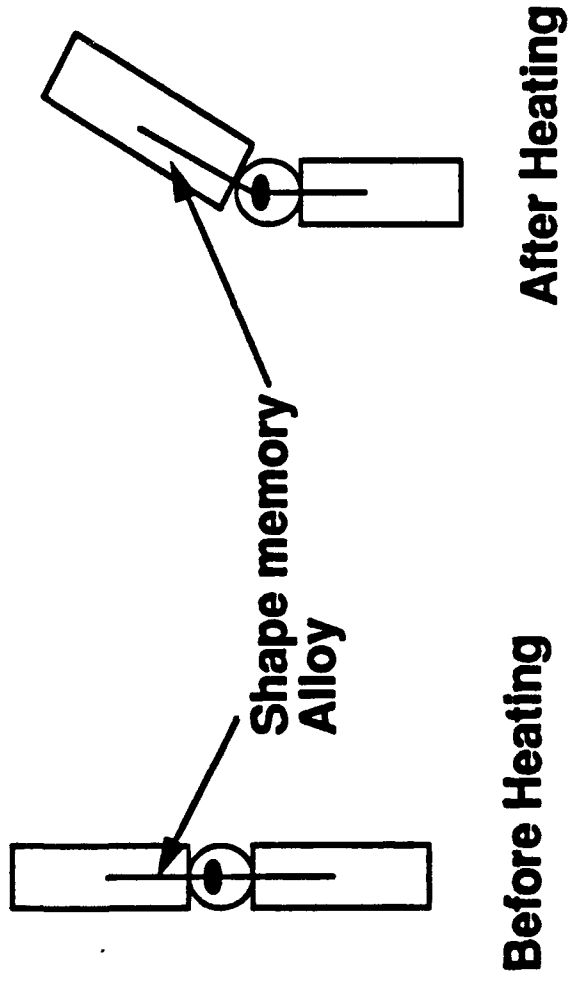
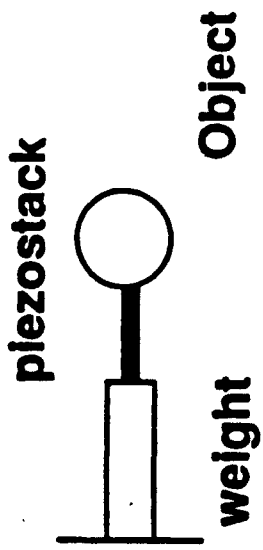
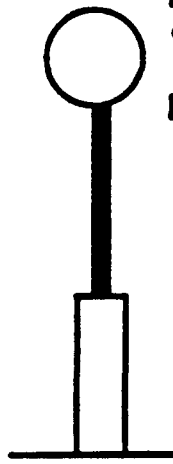


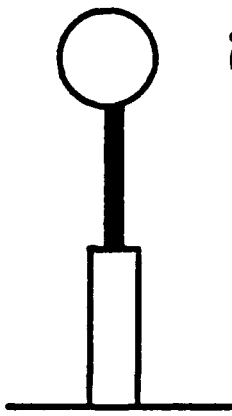
Figure III.3.3 Shape memory alloy as a micromotor.



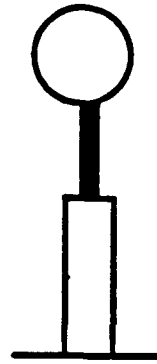
Begin



Fast Expansion



Slow Contraction



New Position

Figure III.3.4 A typical induced drive mechanism.

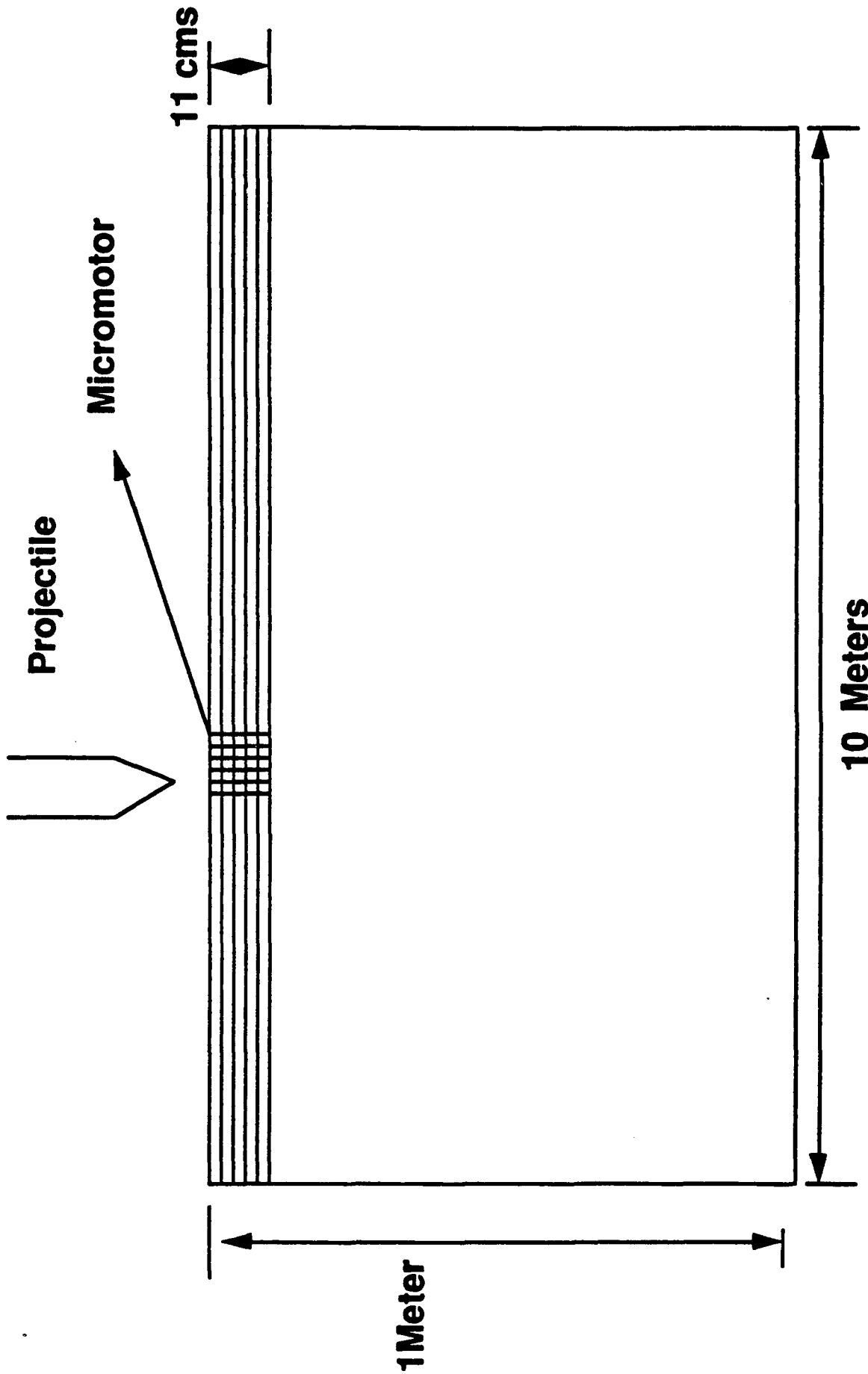


Figure III.3.5 Ceramic plate.

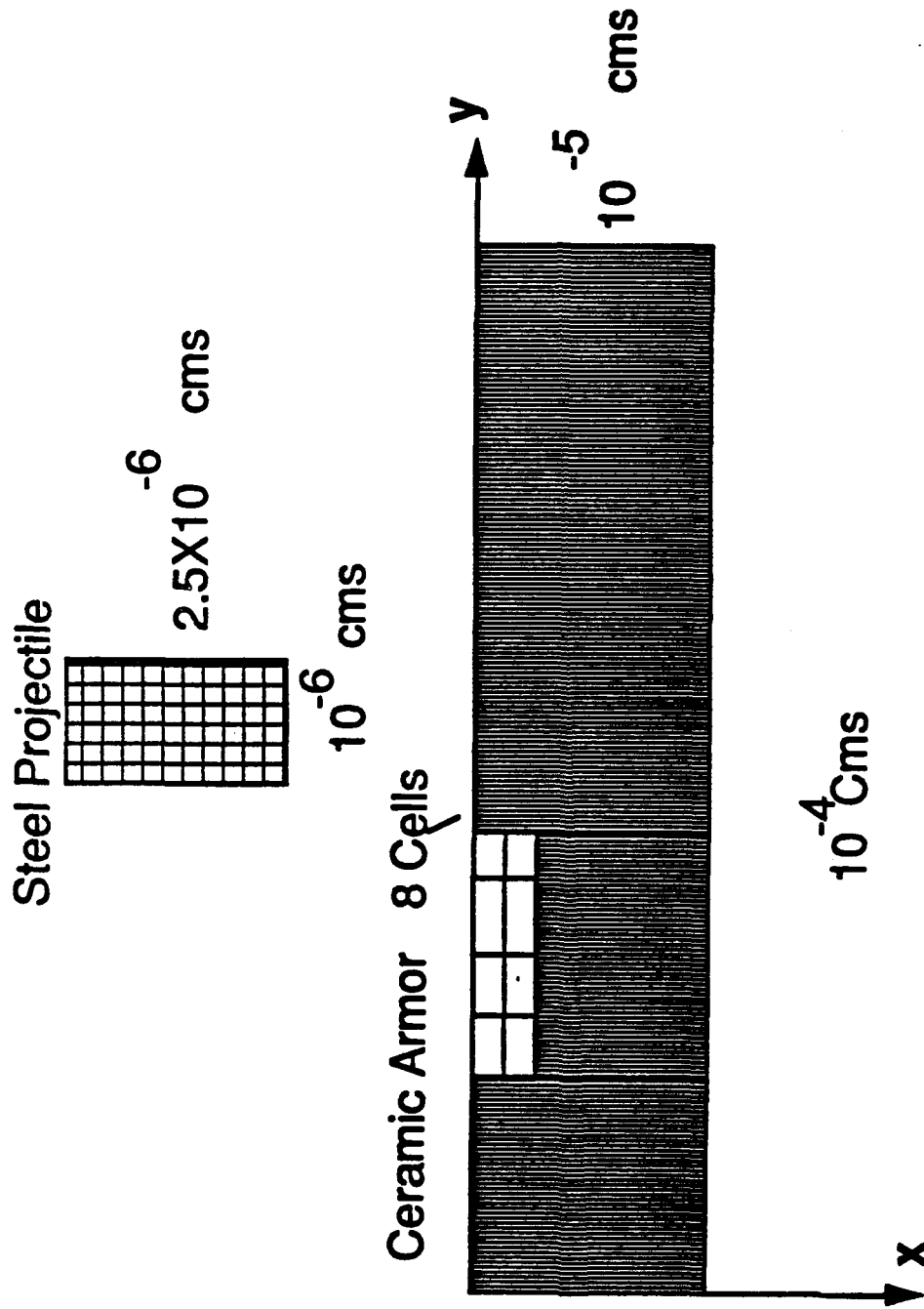


Figure III.3.6 Setup for the microactuation.

1 st Cycle

v_x = velocity in x-direction } in km/sec
 v_y = velocity in y-direction }

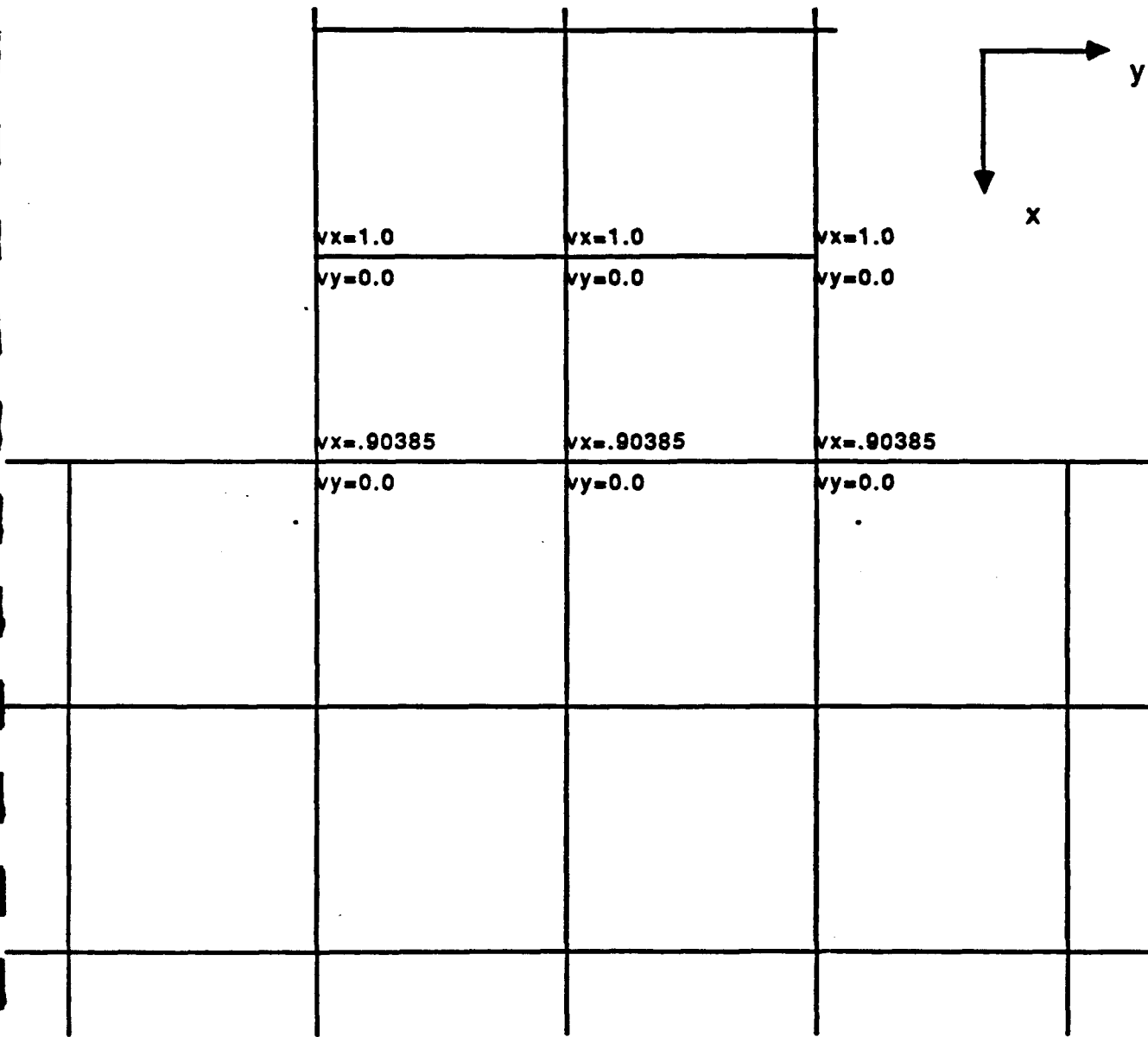


Figure III.3.7 Distorsion plot after first cycle.

10 th Cycle

vx = velocity in x-direction }
 vy = velocity in y-direction } in km/sec

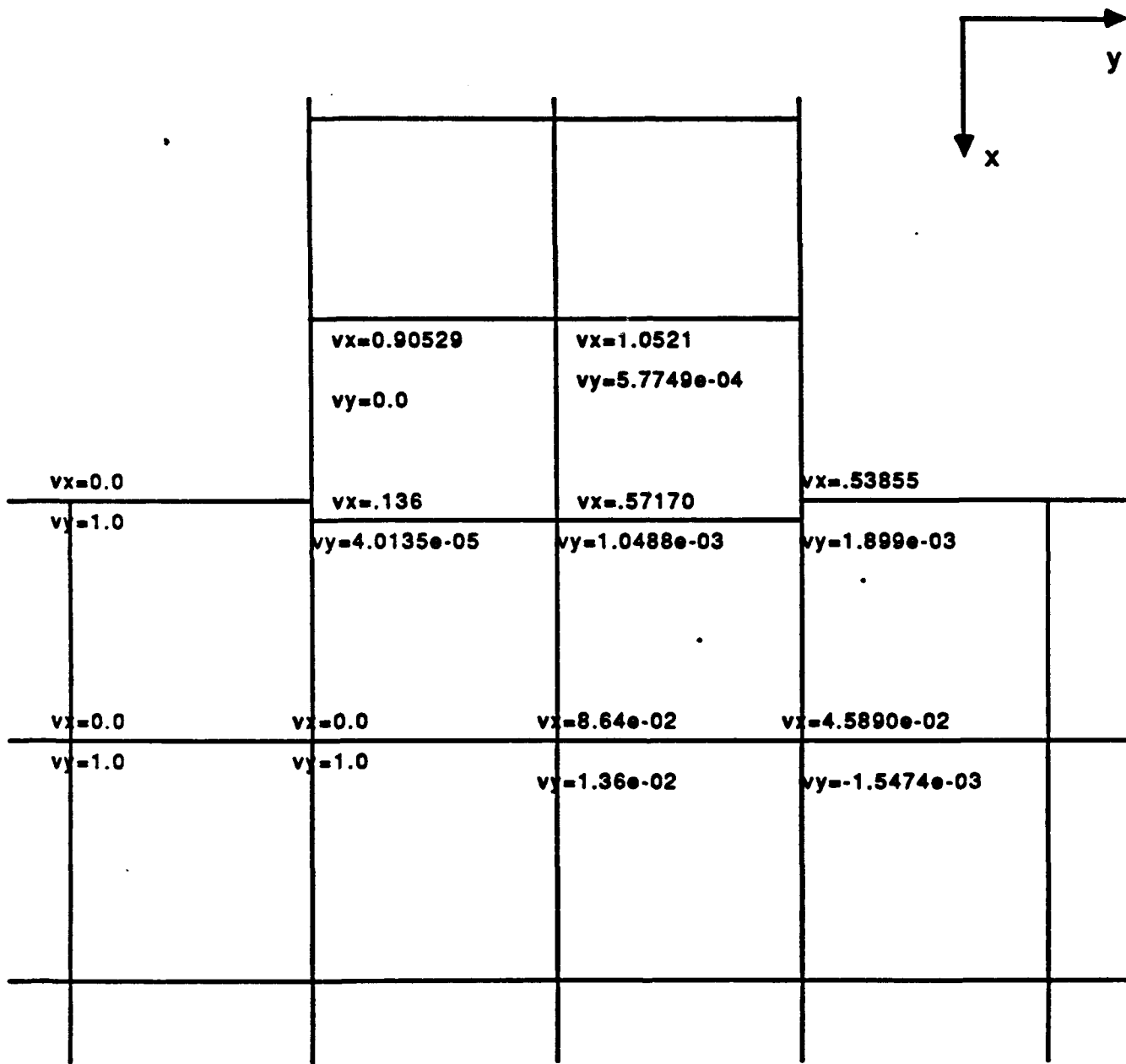


Figure III.3.10 Distortion plot after ten cycles.

III.4 Smart Armors to Defeat Projectiles

Some tank armors are designed with different but fixed sloping surfaces (Figure III.4.1). The purpose of such a design is to deflect the incoming projectile. A projectile with an incident angle normal to the target is capable of optimally channeling the energy into penetrating the target. Depending on the mechanical properties of the target and projectile impact velocity, there is a critical angle of oblique incidence. If this critical angle is exceeded, the projectile is deflected and penetration is prevented.

Armors, with different but fixed slopes, are passive devices. Such armor will not always be able to prevent penetration of projectiles. Projectile builders and users can overcome the passive devices by impacting at different angles of attack. However, a well designed active device can deflect projectiles that impact at varying angles of attack. The active device will be designed to rotate and change the angle of attack. The amount and direction of rotational motion required will be determined on the basis of sensed information.

III.4.A Sensors and Actuators

For such active control, we need sensors that are capable of sensing the angle of attack and the velocity of the projectile. Such determining will be accomplished by using sensors that are capable of sensing the impact velocity and the direction of impact at least 1/100 of a second before impact. This information is based on presentations by B.R.L and John Taylor at the ARO sponsored workshop on Smart Armors.²⁸ The sensed information will be used to determine the amount and direction of the needed rotation to deflect the incoming projectile. This information will be used to trigger an actuator to rotate the armor.

Because of the time constraints, we need sensors and actuators that can respond in microseconds. We should be able to release a hinge, rotate the armor freely by the desired angle and then lock the hinge again. A smart material such as an electrorheological fluid hinge is one of the candidate materials.

III.4.B Electrorheological Fluids in Smart Armor

Electrorheological (ER) fluids were first discovered by Winslow in 1949²⁹. He realized that certain fluids have the ability to significantly alter their rheological properties with the application of an electric field. A typical ER fluid consists of finely divided particles suspended in a non conducting liquid. With the application of an electric field, this liquid system transforms into a semi-solid or a solid system capable of withstanding high shear stresses. The process is reversible. That is, by using electric fields, the load carrying capacity of the ER fluid can be altered. It is this property of the ER fluid that has

been successfully used in an ER Brake ³⁰. We can use this property in the smart armor to defeat the incoming projectile.

A typical control mechanism that can be used for deflecting the incoming projectile is shown in Figure III.4.2. Ceramic armor shields are attached to the military vehicle at critical locations inclined at an angle as shown in Figure III.4.2. For a particular situation, there is a critical angle of incidence, θ_c . When impacted by the incoming projectile at this angle of incidence, the armor will deflect the projectile. It is the objective of the controller to rotate the armor actively to that particular critical angle, θ_c , that depends on the sensed information about the incoming projectile. The armor is hinged to the vehicle at an angle. The hinge consists of ER fluid and is part of the feedback control loop shown in Figure III.4.3. Sensors located in the armor determine the relative angle between the incoming projectile and the armor shield. This information is transmitted to a properly designed controller. The voltage output of the controller is transmitted to the ER fluid hinge. With the application of this voltage, viscosity of the fluid changes and the hinge is released resulting in a relative change in the angle between the projectile and the armor. Because this control mechanism is through an active feedback loop, it can even defeat a smart projectile that is programmed to change the angle of attack as it approaches the target. The governing equations for the plant and sensor are shown in Figure III.4.3 along with the block diagram.

III.4.C E-R Fluid Tests

In order to evaluate the rapid actuation capabilities of E-R Fluids, we conducted some tests. Tests were conducted at the facilities of Triangle Research Inc., Raleigh, North Carolina. We used the micro-encapsulated E-R fluid manufactured by Triangle Research Inc.

Objectives of the tests were to determine the time involved in locking or unlocking a given hinge. We attached a probe similar to the one shown in Figure III.4.4 to a shaker. The metallic probe was immersed in the E-R fluid placed in a beaker. The shaker was actuated to simulate the free motion of the hinge. During the motion of the shaker, an electric field was imposed on the ER fluid. The tests were videotaped. As the electric field was imposed on the ER fluid, the ER fluid became a solid. Then the shaker, probe, ER fluid and the beaker moved as one unit indicating the perfect locking of the hinge. As the electric field was removed, the probe again started moving freely in the fluid.

In our tests, the response time was in milliseconds. By changing the design of the fluid, it is possible to lower the response time to the microsecond range. This is considered a

research issue. Other research issues include sensing capability, design of controllers and model demonstrations.

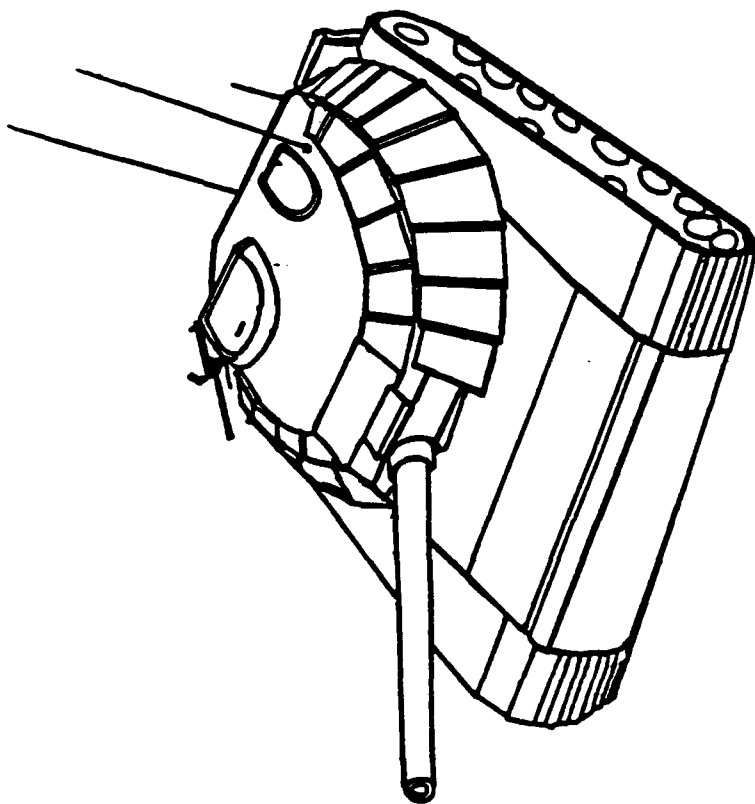
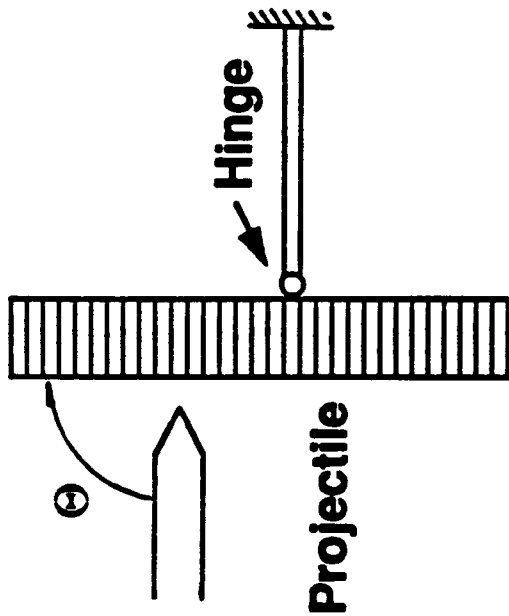


Figure III.4.1 A military vehicle with sloping armor.

Armor Shield



Armor Shield

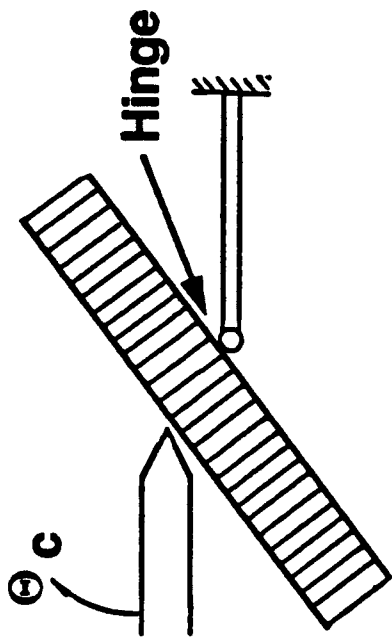
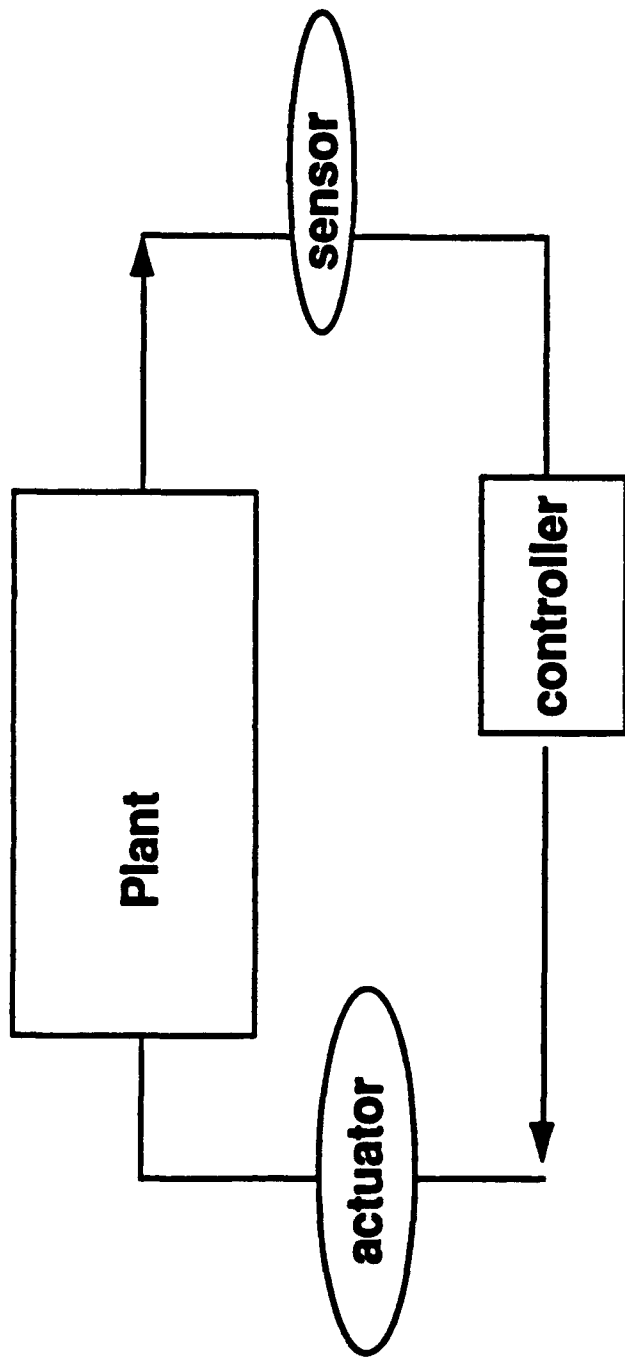


Figure III.4.2 A control mechanism

Θ = Relative angles between armor and projectile
 $M(t)$ = Moment applied to the ER Fluid Hinge
 V = velocity of the incoming projectile



Plant Equations : $I\ddot{\Theta} + C\dot{\Theta} + K\Theta = M(t) \quad \Theta \in \mathbb{R}^3$

Sensor equation : $f(V, \Theta)$

Figure III.4.3. Block diagram.

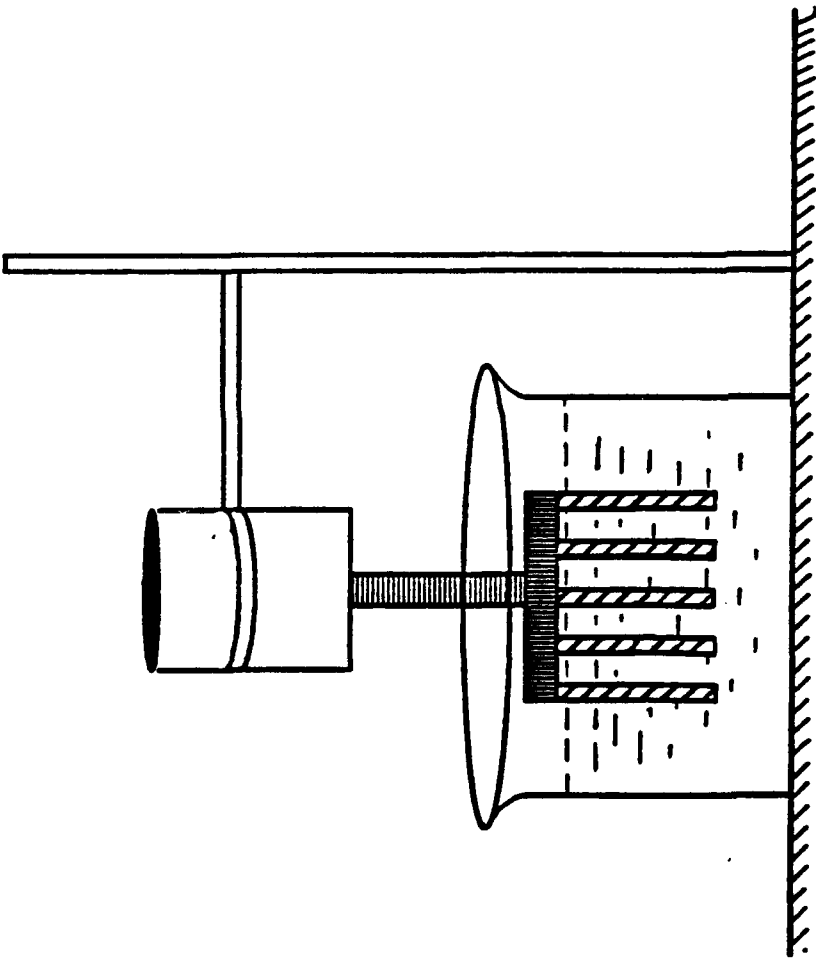


Figure III.4.4 An experimental setup for ER-fluid.

III.5 Smart Reacting Armor

The traditional reactive armor has a layer of explosives on the surface of the armor. The purpose of the explosive is to react to the incoming projectile and defeat the projectile. However, builders of most projectiles have found an easy solution to overcome such a device. The new set of projectiles are designed in two stages (Figure III.5.1). The first stage is a thin dummy projectile. Following the destruction of this first stage, the powerful second stage penetrates the armor.

Our objective will be to design a smart armor to defeat the second and subsequent stages also. We would like to consider a layered concept for smart armor. The design will be accomplished by embedding directed shock wave generators in microbubbles. These microbubbles will be located in selected layers. The directed shock waves will be used to actively change the direction of the momentum of the incoming projectile. The directed shock wave will be generated by using a combination of explosives, solid plates, and foamed metals or graphite to simulate nonlinear springs. Our feasibility studies and past experience have provided the needed foundation for exploring such a design.

In Figure III.5.1, we have discussed a smart reacting armor with microbubbles in the second and third layers of the armor. These microbubbles that can generate a shock wave that will be activated by a controller. Sensors can be located on the top layer of the armor. The sensors can also be embedded inside the armor in an array. The sensed information will be used to select the microbubbles that should be triggered to create a shock wave in the desired direction.

As shown in Figure III.5.2, the shape of the explosively driven pulse can be changed by using a combination of metal and foamed metallic (or graphite) solids that simulate nonlinear springs. For example, it is possible to approximate step function force for a short duration of time.

The change of direction of the reacting unit in the microbubble is needed to focus the shock wave in the direction of the impacting and penetrating projectile. Such changes in the direction of the reacting unit, prior to explosive detonation, will be accomplished by micromotors. The actuation of the micromotors will again be dictated by the controller.

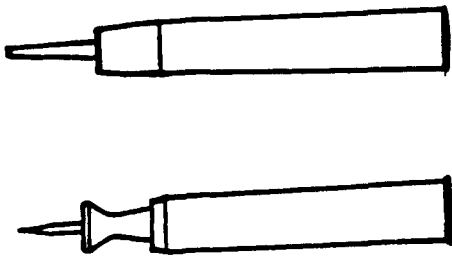


Figure III.5.1 Two stage projectile.

Application of Microactuation Concepts in Smart Armor

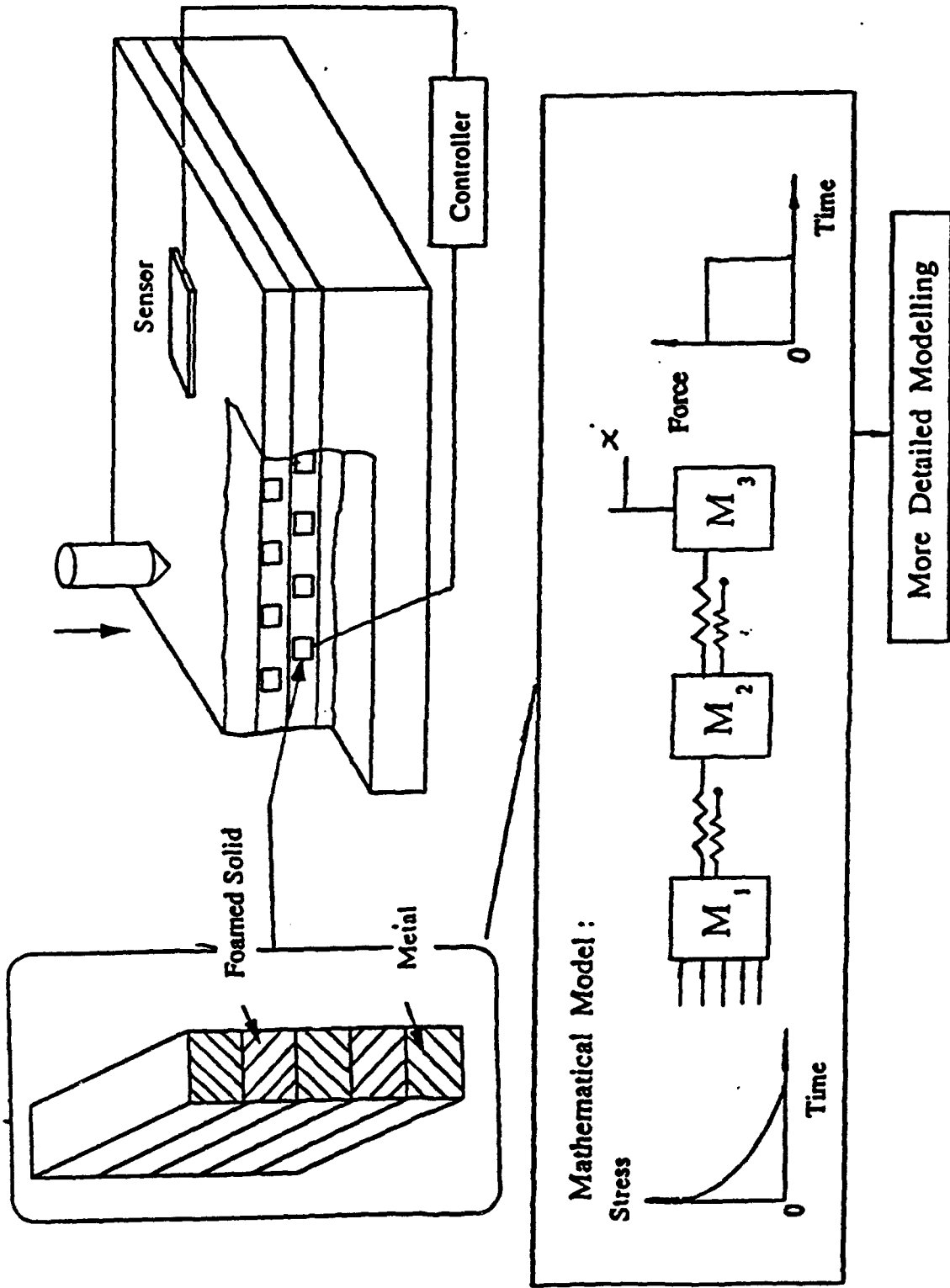


Figure III.5.2 Application of micro-actuation concepts in smart armor.

III.6 Energy Absorption Structure

Enhanced energy absorption by specific portions (perhaps layers) of a multi-component (multi-layer) armor structure may be profitably used in an overall scheme for improved projectile defeat. It is envisioned that one or more layers may be tailored to specifically absorb energy in an essentially passive, but intelligent, fashion, thus relieving other parts of the intelligent armor structure from dealing with the full momentum of the penetrator. The rationale applied in this concept depends upon using as many intrinsic properties of one or more materials, probably comprising a reasonably sophisticated composite structure, in unique ways to absorb and, therefore, dissipate the projectile's energy in as small a volume of the armor structure as possible. The use of ceramic materials which are currently of interest in armor technology is probable, since the properties which make them potentially attractive in standard armor configurations, are likely to be similarly required in these more sophisticated structures.

In armor materials the kinetic energy of an impacting projectile is dissipated in a number of ways. A significant portion of the energy is absorbed during fracture. Another form of energy dissipation is in the form of heat generated by friction, resulting in a temperature rise. Additional forms of energy absorption can likewise be envisioned. Pursuit of improved armor concepts must consider means of maximizing the energy conversion/absorption process in a minimal volume of armor material.

The principal concept considered here is that phase transformations and phenomena resulting from a phase change may be useful in enhancing energy dissipation capabilities.

One or more layers of a multi-layer armor structure may be specifically tailored to enhance particular absorption mechanisms. An embodiment of this concept would be to use a porous matrix or framework of a tough material infiltrated with a relatively low melting material. The low melting material would be intended to experience sufficient temperature rise in the course of the impact event, that it would undergo melting. This would result in maximum energy absorption in the minimum volume, as a result of the absorption of the heat of fusion of the material undergoing melting. This would generally be expected to result in an energy absorption equivalent to that experienced when the solid is heated in a volume several times smaller. Thus the volume involvement in the armor may be minimized.

It is further envisioned that the liquid now formed in a three-dimensional porous network structure, a part of which is likely to remain intact and contain liquid infiltrant rather than solid material, will be forced to flow in the constricted space of the porous structure. The liquid flow will represent an additional

mechanism of energy absorption which can be envisioned as material being squeezed from the matrix like water from a sponge. Obviously the melting point, heat of fusion, melt viscosity and rheology of the molten material will be factors which must be considered in the context of choosing the infiltrant material.

The rheology of the liquid would be considered as perhaps the most influential property in determining the flow characteristics during impact. The high strain/shear rate environment associated with kinetic impact phenomena is not generally considered in the context of rheology. It would be better to perform actual experiments in such an environment (or a high strain rate environment produced by a means other than that possible in a ballistic impact) in order to characterize the behavior of liquids under these conditions.

The matrix material also plays a substantial role in such a scenario, and it is likely that a porous titanium diboride or similar material already considered for armor applications could serve in this function.

Incorporation of concepts such as those considered here into conceptual designs described elsewhere in this report (such as the Vascular Network) are also important. The molten material resulting from impact could be a contributor to the repair mechanisms envisioned in such concepts. It may be feasible to use the resolidifying melt as a component of the repair mechanism.

It is necessary to understand the partitioning of energy absorption during ballistic impact into separate components; such as that associated with fracture or temperature rise. The choices of both the matrix (or matrices if multiple layers are considered) and the infiltrant materials which are optimum depend entirely on considerations such as the range of temperatures which will be encountered in ballistic events. Once the temperature range of interest is known, it will be necessary to identify the material properties which are of importance, and subsequently a number of possible candidate materials. A number of experiments would be necessary, along with modelling approaches, to understand the relative contribution of properties such as heat of fusion, viscosity, and dilatancy (or other rheological behaviors). In parallel, a systematic evaluation of the matrix materials would have to be undertaken, leading to definition of the required characteristics for an optimum matrix material and geometry.

III.7 Dilatant Material

Deformation properties of a composite materials could be tailored to behave in a dilatant fashion by appropriate selection of a low melting material in the system described in the preceding section. Dilatancy could potentially enhance the resistance of a material to penetration as a result of the high liquid viscosity

associated with the shear stress during the impact event. The movement of the liquid being forced out of the network porosity would be inhibited, thus allowing rapid energy dissipation as heat. The liquid would tend to remain in the vicinity of the damage allowing it to resolidify in place thus affecting repair. The latter function is envisioned to occur while the liquid is still present but after the high shear stress associated with the ballistic impact has ended. The liquid viscosity would need to drop sufficiently to allow flow into the damaged area.

III.8 Broken Shells

The main effort on the broken shells portion of the program was conceptual in nature. Of primary interest was the timely demonstration of the principle behind the idea using polymeric materials such as epoxies and resins, and later, the search for material systems more suitable to armor applications. The polymeric based systems can function as the initial input to a first generation computer model.

Figure III.8.1 shows a cross section of the structure of the broken shell concept. In the initial proof of concept portion of the program the shell skin can be made of either a thin polymeric membrane or a thin relatively low strength glass. At this stage the shell will not be structural in nature. It serves to maintain the reacting species apart. One of the species is contained in the shell, and the other in the interstitial space. The reacting species may be simply a monomer and its initiator. When the shell breaks initiator is released and begins rapid polymerization of the monomer in the adjacent area. The amount of polymerization would depend on the amount of damage, ie. the more shells are broken, the more initiator is released thereby causing more monomer to polymerize. In the ideal case the reaction product material will be less dense than the reactants. The effect would therefore tend to replace material volume lost in the impact. Testing and modelling will probably begin with methyl methacrylate and benzoyl peroxide as the reactants and poly methyl methacrylate (plexiglas) as the product material. This material system was chosen due to its familiarity, availability, and the ability to vary the polymerization rate with initiator concentration.

A modification to the broken shell concept would encapsulate both of the reactants in shells and fill the interstitial space with a structural material. The modified geometry may prove superior in structural integrity, due to the interstitial support structure, and control of the ratio and location of reactant release. The shells may be made of two different sizes each containing, respectively, the ideal volume of monomer and initiator. When the shells are broken monomer and initiator are released in a localized area in approximately the proper ratio.

The advantages of this system is its simplicity of operation once fabricated and installed. There are no systems to monitor, nor must a response to damage be initiated by the crew or computer. The response is inherent in the structure and material system. A disadvantage is that the amount of reactants is finite and specifically located in the structure. If damage is above a certain threshold there will not be enough material to completely refill the void, and once a specific location is damaged and self-repairs, further damage to that location cannot be repaired.

III.9 Vascular Network

Initially the vascular network concept is envisioned to be similar to the broken shell concept. The matrix material will be mainly structural in nature, however it will contain discreet amounts of initiator. Figure III.9.1 shows the system in its most basic proof of concept form. The thin glass tubes are filled and pressurized with a liquid monomer which polymerizes when it comes in contact with the initiator in the matrix. When damage is incurred one or more of the tubes will break causing the monomer to escape and begin repairing the damage. When the system senses a pressure loss in the tubes, pumps are activated, draw monomer from a reservoir, and increase the amount and pressure of monomer being expelled to fill the voids and cracks in the armor. When the monomer polymerizes, the tube will be resealed and the consequent pressure increase would cause the pumps to reduce pressure in the tubes to the normal standby state.

The vascular network has an advantage over the shell concept in that the amount of monomer is no longer limited to that in the immediate area. The tubes can deliver monomer from a reservoir to the damaged area from considerable distance. However, the amount of initiator is still limited. The result may be that in heavily damaged areas monomer may continue to seep until the reservoir is emptied.

More advanced systems could have the monomer and initiator flowing in separate, but adjacent tubes. This would ensure a continuing supply of initiator. If the tubes are in physical contact with each other, a shock would break both tubes at, relatively, the same time releasing monomer and initiator. The dual tube system should be able to repair larger volumes than the broken shell or single tube systems because reactants can be transported to the damage site from other locations. As with the single tube system damage to the tubes would cause a pressure loss thereby activating the reservoir pumps. When the damage is repaired the tube pressure will increase and the pumps will reduce to normal standby pressures. Positive pressure in the dual tubes should prevent polymerization from blocking flow through the tubes and may result in regrowth of severely damaged tube sections.

BROKEN SHELLS

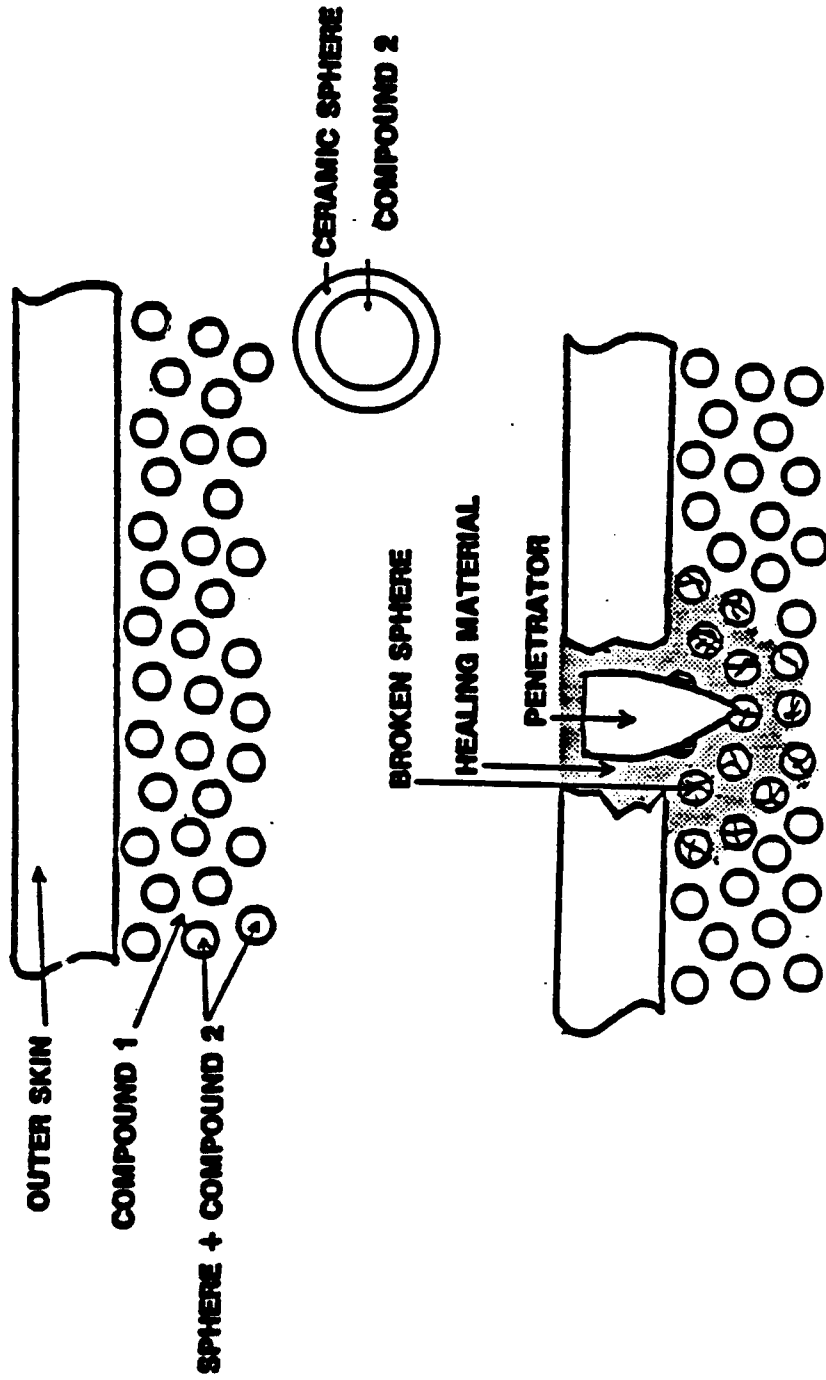


Figure III.8.1

VASCULAR NETWORK

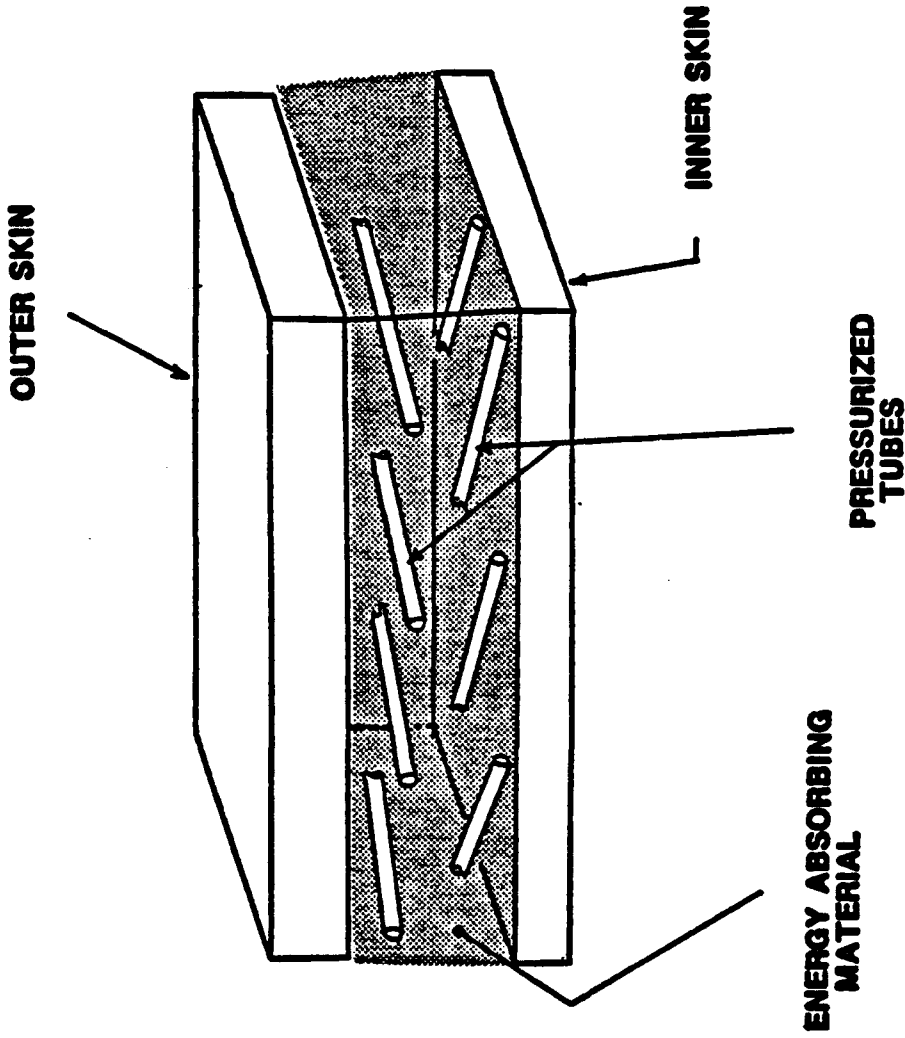


Figure III.9.1

III.10 Electromigration

Electromigration is a process of material transport which occurs as a result of an electric current passing through a conductor. It is dependent upon the current density, thus being enhanced by a reduction in conducting cross-section which increases the local current density. It is conceptualized that the process could be used to repair damage in a structure by providing a mechanism for transfer of material into voids and cracks created during penetration.

The system would be designed to detect the area of impact and respond by application of a voltage resulting in the flow of adequate current through the damaged region to promote the transfer of material. The electromigration process is enhanced by increasing temperature, thus it might be expected, fortuitously, to proceed most rapidly in the region affected by the impact.

IV. LIST OF PARTICIPATING SCIENTIFIC PERSONNEL

- K. V. Logan, Co-Principal Investigator
- S. N. Atluri, Co-Principal Investigator
- S. V. Hanagud, Co-Principal Investigator
- W. L. Ohlinger, Senior Research Engineer
- G. R. Villalobos, Research Engineer II (PhD student, Materials Engineering)
- G. Pan, PhD student, Mechanics
- Y. Kitajima, PhD student, Mechanics
- G. L. Nagesh-Babu, PhD student, Aerospace Engineering
- S. Shamanna, PhD student, Aerospace Engineering
- D. P. Piotrowski, Undergraduate student, Materials Engineering

VI. RECOMMENDATIONS

The following are recommendations for further development:

1. Improve the penetration code: To include fracture mechanics and internal boundary conditions; calculations with embedded sensors and actuators; closed loop simulation; inclusion of different types of restraints.
2. Calculation of forces needed to provide constraints.
3. Parametric modeling studies of penetration, including: Velocity of projectile, various projectile materials, size and shape of projectile and target, target boundary conditions.
4. Further determine the feasibility of sensor concepts including the following:
 - (a) Detailed analysis of sensor performance requirements, e.g., sensitivity, output requirements, etc.
 - (b) Identification of candidate sensor materials and systems for incorporation of promising materials into structures.
 - (c) Identification of research issues resulting from unfulfilled sensor requirements.
 - (d) Research and development of suitable sensor materials, materials processing and techniques for incorporation into armor systems.
5. Micromotors and piezoceramic actuators including:
 - (a) Detailed analysis of actuator performance requirements, e.g., torque (micromotors), linear force, drive requirements, response times, activation speeds, range of motion, etc.
 - (b) Identification of candidate materials and their limitations, development of materials to provide required performance, development of fabrication technology, development of means of integration into armor materials systems.
 - (c) Identification of controller related issues and design of controller systems.
 - (d) Actuator design and optimization of location.
6. Evaluation of electrorheological fluid systems concepts including:

- (a) System configurations.
 - (b) Feasibility of achieving required response times.
 - (c) Control and actuation requirements.
7. Design and construction of test articles with embedded actuators and sensors.
 8. Experiments to illustrate feasibility of sensor/actuator concepts including integration into armor prototype structures.
 9. Analysis of impact phenomena to identify partitioning of energy absorption/dissipation among active mechanisms, such as fracture, thermal effects, etc.
 10. Evaluation of relative energy absorption capacities of porous infiltrated systems considering fracture, thermal effects, phase transformations, abrasion, etc.
 11. Fabrication and testing of prototype structures incorporating unique energy absorption mechanisms.
 12. Consideration of detailed designs incorporating layered structures with layers tailored to optimum performance of particular functions relative to projectile condition, velocity and energy (or momentum).
 13. Fabrication and testing of prototype "healing" systems to include identification of candidate material systems compatible with armor requirements.

BIBLIOGRAPHY

1. Roger, C. A. Rogers, U.S. Army Research Office Workshop on Smart Materials, Structures and Mathematical Issues Blacksburg, VA, September 15-16 1988.
2. Newham, R. E., and G. R. Ruchau, "Smart Electroceramics", Journal of the American Ceramic Society, 74, 463-480, (1991).
3. Yatteu, J. D. and Wisotski, J. (1981), "Penetration of Fluids by Rod Type Projectile", Sixth International Symposium on Ballistics, Orlando, FL (27-29 October, 1981).
4. Kinslow, R., High Velocity Impact Phenomena, Academic Press (1970) New York and London.
5. Msc-Pisces - 2DELK, Users Manual, Msc Corporation, 1991.
6. Trimmer, W. S. N. and K. J. Gabriel, "Design Considerations for a Practical Electrostatic Micromotor," Sensors and Actuators, 11, 1987, pp. 1899-206.
7. Moore, A. E., "Electrostatics and Its Applications," John Wiley & Sons, 1973.
8. Fan, L. S., Tai, Y-C and Muller, R.S., "IC Processed Electrostatic Micro-Motors", IEEE Int. Electron Devices Meeting, San Francisco, CA, 1988, pp 666-669.
9. Fujimoto, A., Sakata, M., Hirano, M. and Goto, H., "Miniature Electrostatic Motor", Sensors and Actuators, 24, 1990, pp 43-46.
10. Tai, Y.C. and Muller, R.S., "IC-Processed Electrostatic Synchronous Micromotors", Sensors and Actuators, 20, 1989, pp 49-55.
11. Kuribayashi, K., " Millimeter Sized Joint Actuator Using a Shape Memory Alloy", Sensors and Actuators, 20,1989, pp 57-64
12. Higuchi, T., Yamagata, Y., Furutani, K. and Kudoh, K., "Precise Positioning Mechanism Utilizing Rapid Deformations of Piezoelectric Elements", IEEE Proceedings, 1990, pp 222-226
13. Moroney, R. M., White, R. M. and Howe, R.T., "Ultrasonic Micromotors", Ultrasonics Symposium, 1989, pp 745- 748.
14. Jacobsen, S. C., Price, R. H., Wood, J. E., Rytting, T. H. and Rafaelof, M., "A Design Overview of an Eccentric-Motion Electrostatic Microactuator (The Wobble Motor)", Sensors and Actuators, 20, 1989, pp 1-16.

15. Kumar, S., Cho, D., and Carr, W. "A Proposal for Electrically Levitating Micromotors", Sensors and Actuators, 24, 1990, pp 141-149.
16. Jebens, R., Trimmer, W., Walker, "Microactuators for Aligning Optical Fibers", Sensors and Actuators, 20, 1989 pp 65-73.
17. Mahadevan, R., Mehregany, M. and Gabriel, K.J., "Application of Microactuators to Silicon Micromechanics", Sensors and Actuators, 1990, pp 219-215.
18. Bart, S. F. and Lang, J.H., "An Analysis of Electro-quasistatic Induction Micromotors", Sensors and Actuators, 1989, pp 97-106.
19. Pisano, A., "Resonant-Structure Micromotors: Historical Perspective and Analysis", Sensors and Actuators, 20, 1989, pp 83-89.
20. Trimmer, W. and Jebens, R., "Harmonic Electrostatic Motors", Sensors and Actuators, 20, 1989, pp 17-24.
21. Ibid 3.
22. Ibid 5.
23. Ibid 6.
24. Ibid 7.
25. Ibid 8.
26. Ibid 8.
27. Ibid 10.
28. Workshop on Smart Materials for Resilient Structures, Research Triangle Park, Sept. 1991.
29. Winslow, W.M., "Induced Vibrations of Suspensions", J. Applied Physics, 1949, pp 1137-1140.
30. Colman, D Triangular Research Inc., NC, Personal communication, 1992.